aerodyne research, inc.

ARI-RR-105

A CW HF LASER WITH SUPERSONIC PREMIXING AND STATIONARY SHOCK INITIATION

(Final Report)

by

James P. Moran
Charles E. Kolb

Sponsored by Defense Advanced Research Projects Agency
DARPA Order No. 3012

This research was supported by the Defense Advanced Research Projects Agency of the Department of Defense and was monitored by the Office of Naval Research under Contract No. N00014-75-C-1123

April 1977

bedford research park, crosby drive, bedford, massachusetts 01730 (617) 275-9400

The views and conclusions contained in this document are those of the author and should not be interpreted as necessarily representing the official policies, either expressed or implied, of the Defense Advanced Research Projects Agency or the U.S. Government.

UNCLASSIFIED

SECURITY CLASSIFICATION OF THIS PAGE (When Data Entered)

REPORT DOCUMENTATION PAGE

READ INSTRUCTIONS BEFORE COMPLETING FORM

1. REPORT NUMBER

2. GOVT ACCESSION NO.

3. RECIPIENT'S CATALOG NUMBER

4. TITLE (and Subtitle)
A CW HF Laser With Supersonic Premixing and Shock Initiation

5. TYPE OF REPORT & PERIOD COVERED
Final Report
6/1/75 - 12/31/76

6. PERFORMING ORG. REPORT NUMBER
ARI-RR-105

7. AUTHOR(s)
James P. Moran
Charles E. Kolb

8. CONTRACT OR GRANT NUMBER(s)
N00014-75-C-1123
DARPA Order-3012

9. PERFORMING ORGANIZATION NAME AND ADDRESS
Aerodyne Research, Inc.
Bedford Research Park, Crosby Drive
Bedford, MA 01730

10. PROGRAM ELEMENT, PROJECT, TASK AREA & WORK UNIT NUMBERS
Order No. 3012

11. CONTROLLING OFFICE NAME AND ADDRESS
Defense Advanced Research Project Agency
1400 Wilson Blvd.
Arlington, VA 00090

12. REPORT DATE
April 1977

13. NUMBER OF PAGES
57

14. MONITORING AGENCY NAME & ADDRESS (if different from Controlling Office)
Office of Naval Research
Washington, D.C. 20375
Joseph Stregack, Monitor

15. SECURITY CLASS. (of this report)
Unclassified

15a. DECLASSIFICATION/DOWNGRADING SCHEDULE

16. DISTRIBUTION STATEMENT (of this Report)

DISTRIBUTION STATEMENT A
Approved for public release;
Distribution Unlimited

17. DISTRIBUTION STATEMENT (of the abstract entered in Block 20, if different from Report)

18. SUPPLEMENTARY NOTES

19. KEY WORDS (Continue on reverse side if necessary and identify by block number)

HF Laser
CW Chemical Laser
Stationary Shock Wave
Stationary Detonation Wave
Premixed Chemical Laser
Resonance Fluorescence
Chemical Production of Factors

20. ABSTRACT (Continue on reverse side if necessary and identify by block number)

Formation of HF by the chain reaction is initiated by the simultaneous reaction $NO + F_2 \rightarrow NOF + F$. A detonable mixture of the reactants, H_2, F_2, and NO in argon or helium diluent, is achieved by secondary injection of H_2 and NO along the trailing edges of a two-dimensional nozzle array into a cold supersonic stream of premixed F_2 plus diluent. Mixing of the secondary injectants is achieved without significant chemical reactions in a slightly divergent supersonic mixing section. The resultant detonable mixture is directed into a chamber as a slightly underexpanded free jet. This free jet

DD FORM 1 JAN 73 1473 EDITION OF 1 NOV 65 IS OBSOLETE

UNCLASSIFIED

SECURITY CLASSIFICATION OF THIS PAGE (When Data Entered)

390 112

Abstract (Cont.)

is interrupted shortly downstream of its exit plane by a nearly normal shock wave. The shock is held in a stationary manner by a shock holder which accepts only a portion ($\approx$ 70%) of the total jet flow. An adjustable sonic throat, within the shock holder, controls the accepted fraction. Laser mirrors in a fixed stable-cavity configuration constitute two walls of the shock holder. Maximum laser cavity intensity, sampled through several small holes in one mirror, presently appears to be in excess of 51 w/cm^2, as deduced from measurements of power in excess of 117 mw incident on a PbSe detector. Laser power output in excess of 20w, in a closed cavity configuration, was determined from local mirror heating by thermocouple measurements. This work represents the first success in achieving a stationary shock in a detonable mixture in a configuration other than a free jet. Furthermore, it represents the first demonstration of CW laser operation across a stationary shock.

TABLE OF CONTENTS

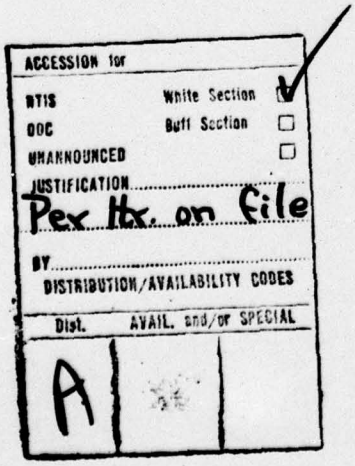

LIST OF ILLUSTRATIONS

A CW HF laser with supersonic premixing and stationary shock initiation†

BY JAMES P. MORAN

Aerodyne Research, Inc., Bedford, Massachusetts 01730

- ABSTRACT -

Formation of HF by the chain reaction is initiated by the simultaneous reaction $NO+F_2 \longrightarrow NOF + F$. A detonable mixture of the reactants, H_2, F_2, and NO in argon or helium diluent, is achieved by secondary injection of H_2 and NO along the trailing edges of a two-dimensional nozzle array into a cold supersonic stream of premixed F_2 plus diluent. Mixing of the secondary injectants is achieved without significant chemical reactions in a slightly divergent supersonic mixing section. The resultant detonable mixture is directed into a chamber as a slightly underexpanded free jet. This free jet is interrupted shortly downstream of its exit plane by a nearly normal shock wave. The shock is held in a stationary manner by a shock holder which accepts only a portion ($\simeq 70\%$) of the total jet flow. An adjustable sonic throat, within the shock holder, controls the accepted fraction. Any fraction less than that which corresponds to supersonic entry will force the occurrence of a normal shock slightly upstream of the shock holder inlet. Shock standoff distance is coupled to accepted fraction, and back pressure in the free jet chamber is controlled by the rejected flow fraction and blowdown receiver geometry.

Absence of significant chemical reactions in the supersonic mixing section was verified by observations of constant supersonic static pressure and constant postshock temperature during the introduction of fluorine, the final reactant, to the flowing system. Completion of chemical reactions in the shock holder was verified by observations of gas temperature rise between the inlet and the sonic throat. Absence of reactions in the absence of NO verified the chemical initiation of the chain reaction. Schlieren motion picture photography as well as various pressure measurements verified the occurrence of a stationary shock. Laser mirrors in a fixed stable-cavity configuration constitute two walls of the shock holder. Maximum laser cavity intensity, sampled through several small holes in one mirror, presently appears to be in excess of 51 w/cm^2, as deduced from measurements of power in excess of 117 mw incident on a PbSe detector. Laser power output in excess of 20w, in a closed cavity configuration, was determined from local mirror heating by thermocouple measurements.

This work represents the first success in achieving a stationary shock in a detonable mixture in a configuration other than a free jet. Advantages of the present shock holder include high pressure recovery (shock holder pressure/jet exit pressure $\simeq 8$) combined with efficient gas utilization (68% accepted flow fraction). Furthermore, it represents the first demonstration of CW laser operation across a stationary shock.

† This work was sponsored by Navy/DARPA under Contract No. N00014-75-C-1123. The Technical Monitor was Joseph Stregack of the Naval Research Laboratory.

I. INTRODUCTION

Chemically pumped laser radiation has been induced by a traveling detonation wave, as first reported by Gross, et al. (1969), in shock tube studies with mixtures of F_2O, H_2 and Ar. Stationary shock waves have been achieved in premixed detonable gases by several investigators, in various flow configurations. The feasibility of achieving continuous wave laser radiation from a purely chemically pumped $H_2 + Cl_2$ system, in which chemical reactions are initiated in a premixed stream by a stationary shock wave, was examined theoretically by Bowen and Overholser (1969). In their studies, the chain reaction was postulated to be initiated by thermal dissociation of Cl_2. They concluded that the scheme might be pursued with a reasonable expectation of success; however, this has not been demonstrated experimentally. In HF/DF laser systems, atomic fluorine production may be achieved with little chemical heat release by the reaction of nitric oxide with molecular fluorine. This mechanism was used successfully by Cool, et al. (1970) in an HF chemical diffusion laser, but has not previously been considered in a fully premixed CW laser application.

Work reported here describes the first successful demonstration of a chemically pumped CW laser with stationary shock initiation in a premixed detonable gas stream. A new shock holder configuration was employed, which demonstrates high pressure recovery and efficient gas usage. A multiple nozzle/injector array was used to achieve mixing over a large portion of the supersonic stream. Atomic fluorine was produced by the reaction

$$NO + F_2 \longrightarrow NOF + F \qquad k_f = 7.04 \times 10^{-13}\, e^{-1150/T} \quad \text{(Kolb, C., 1976)}$$

Complex nonequilibrium processes in highly exothermic gas phase reactions may be studied most easily in steady flow. Stationary shock initiation of reactions has offered a convenient configuration for such studies, since thorough gas mixing may be achieved in the cold supersonic flow upstream from the shock wave. In detonable mixtures, one has limited options in flow geometries, since the stationary shock must be isolated from the wall boundary layers of the supersonic mixing zone. Three shock configurations have previously been demonstrated: (a) a Mach-disc shock formed by the convergence of the barrel shock in a highly underexpanded supersonic jet (Nicholls, et al., 1958, 1960, 1962); (b) the normal shock produced by Mach reflection of two converging oblique shocks, which emanate from facing wedges in a supersonic wind tunnel (Gross, 1957, Richmond & Shreeve, 1967); and (c) the normal shock produced in an overexpanded two-dimensional jet in which boundary suction was applied at the end of the supersonic mixing section (Suttrop, 1965). In all the above studies, the initiating shock was isolated from the boundary layers of the mixing section. All studies were conducted with preheated air in the main supersonic stream, and fuel injection through a single axisymetric, or linear injector such that only a central portion of the supersonic stream was uniformly premixed. This allowed area relief downstream from the initiating shock to prevent flow choking. These techniques provide a stationary reference frame for studies of chemical kinetics in premixed detonable gases, which is a great improvement over alternatives such as shock tubes, ballistic ranges and pulsed quiescent gas studies. However, in the present application of stationary shock initiation of continuous wave lasers, the above techniques are not appropriate in the light of requirements for

practical devices. A new shock holder configuration is described which is more suitable to this application. Specifically, one requires efficient gas usage and high pressure recovery. When premixing is achieved in a supersonic stream, one would hope to recover a major portion of the flow at a pressure which is large relative to that in the supersonic stream. The stationary shock configuration of Nicholls, et al. (1958, 1960, 1962), would, in principle, remain stable if the major portion of the supersonic stream contained a detonable gas mixture. However, the highly underexpanded jet precludes efficient pressure recovery, and only a small portion of total flow crosses the Mach disc. The stationary normal shock produced by two converging oblique shocks in the studies of Gross (1957) and of Richmond and Shreeve (1967) can produce high pressure recovery. However, to avoid choking in this converging flow geometry, a premixed detonable mixture may exist in only a small central portion of the supersonic stream, thus precluding efficient gas usage. In this sense, this configuration does not, in fact, produce a stationary shock in a detonable mixture. The overexpanded jet configuration of Suttrop (1965) allows flow expansion downstream from the normal shock; consequently, the degree of gas usage may be limited only by the fraction of jet flow which crosses the normal shock. Pressure recovery is limited mainly by the extent to which the jet flow may be overexpanded, hence, by the extent of removal of wall boundary layers. The results reported by Suttrop (1965) show a modest ratio of post shock recovery pressure to supersonic static pressure of 2.82. The shock holder reported here, achieves pressure recoveries typically greater than 7.8 for more than 68% of the total supersonic flow. In the present system, a premixed detonable mixture is directed into a

chamber as a slightly underexpanded free jet. This supersonic jet is interrupted shortly downstream from its exit plane by a nearly normal shock wave. The shock is held in a stationary manner by a shock holder which accepts only a portion of the total jet flow. An adjustable sonic throat, within the shock holder, controls the accepted fraction. Any fraction less than that appropriate for supersonic entry forces the occurrence of a normal shock slightly upstream from the shock holder inlet. Shock standoff distance is coupled to accepted fraction, and back pressure in the free jet chamber is controlled by the rejected flow fraction and blowdown receiver geometry.

Although supersonic mixing of preheated gases has successfully produced detonable compositions in the above referenced works, these were achieved with single secondary fuel injectors to produce air/hydrogen or air/hydrocarbon mixtures. Preheating of fluorine, to produce the atomic species necessary to drive the shock induced chain reaction, would likely require active cooling of the multiple nozzle array which was used in the present work. This complication was overcome by injection of nitric oxide with the hydrogen in the secondary injector array; this produces atomic fluorine downstream from the stationary shock according to the above reaction. The above rate coefficient was measured by Kolb (1976) in an earlier segment of the present work. In this technique, no active heating or cooling of injected species or nozzles was required.

Since the achievement of combustion of a detonable gas mixture across a stationary shock had not previously been demonstrated, either with a multiple nozzle injector array or with the present shock holder configuration, compromises in system design were made to this end which were at some expense to good laser operation.

The resulting device has successfully demonstrated laser power extraction; however, due to its present rigid design, it cannot demonstrate the potential of such a scheme for practical laser application. Selections of fixed cavity optical configurations were based upon theoretical predictions of premixed laser performance employing the RESALE (Adams, et al., 1975) code. Relevant HF laser kinetics were updated in the code according to the recommendations of Cohen and Bott (1976). Relevant NO chemical kinetics include the above atomic species production reaction and the extinguishing reaction,

$$NOF + H \longrightarrow NO + HF \qquad k_f = 10^{-10}\, e^{-500/T} \text{ (cc/sec)}$$

The above rate is a best estimate (Kolb and Kaufman, 1976) based on the measured rates for the reactions

$$NOCl + H \longrightarrow NO + HCl$$

$$NO_2 + H \longrightarrow NO + OH$$

II. EXPERIMENTAL APPARATUS

Major system components are shown in figure 1(a). Diluent (He or Ar) enters the rear of the primary plenum which is rectangular in cross section with inner dimensions 4.0 cm in height and 10.0 cm in width. Diluent flow is divided as a core flow and a shroud flow which are separated by a thin walled conduit of rectangular cross section with dimensions of 2.0 cm in height and 8.0 cm in width. The height of the plenum and core flow conduit taper proportionately to 2.0 and 1.0 cm, respectively

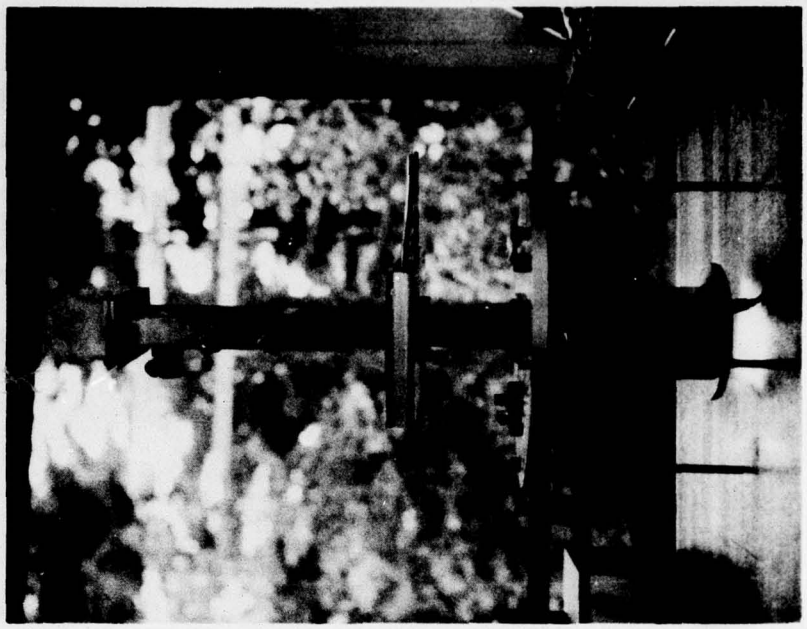

Fig. 1a Assembled Plenum, Nozzle, Mixer, and Shock Holder

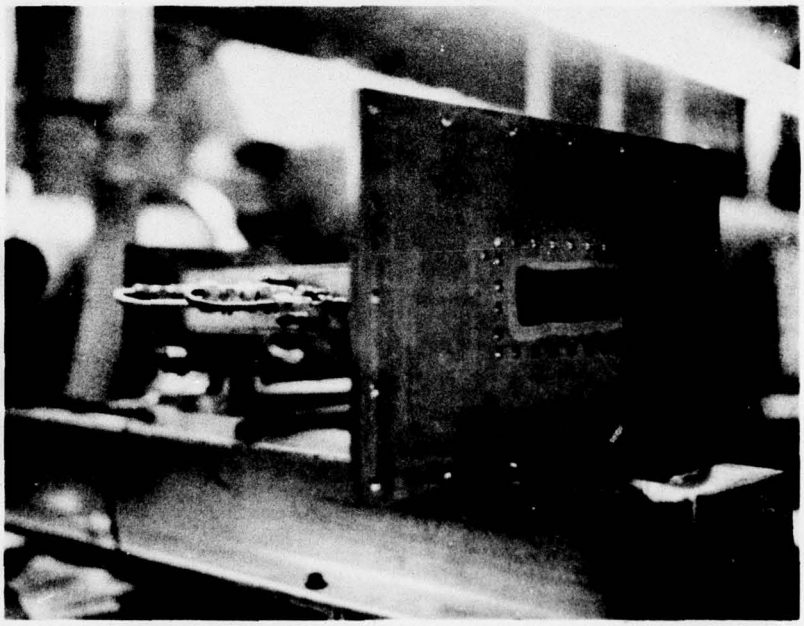

Fig. 1b Plenum With Core Flow Conduit Exposed

Figure 1. Major System Components. AL-1771

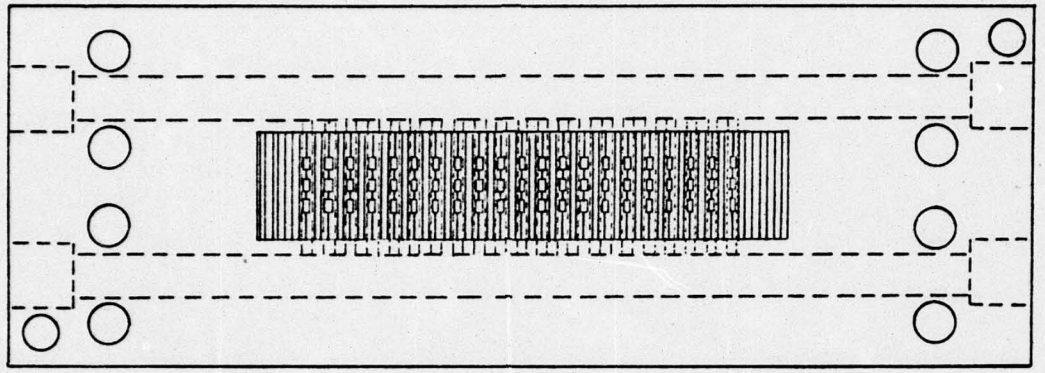

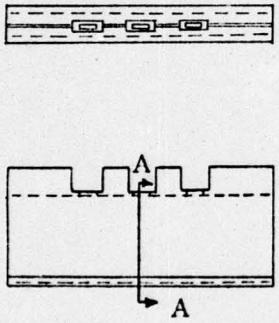

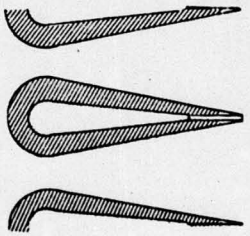

SECTION A - A

Figure 1 c - Nozzle Array

Figure 1 (Continued) - Major System Components.

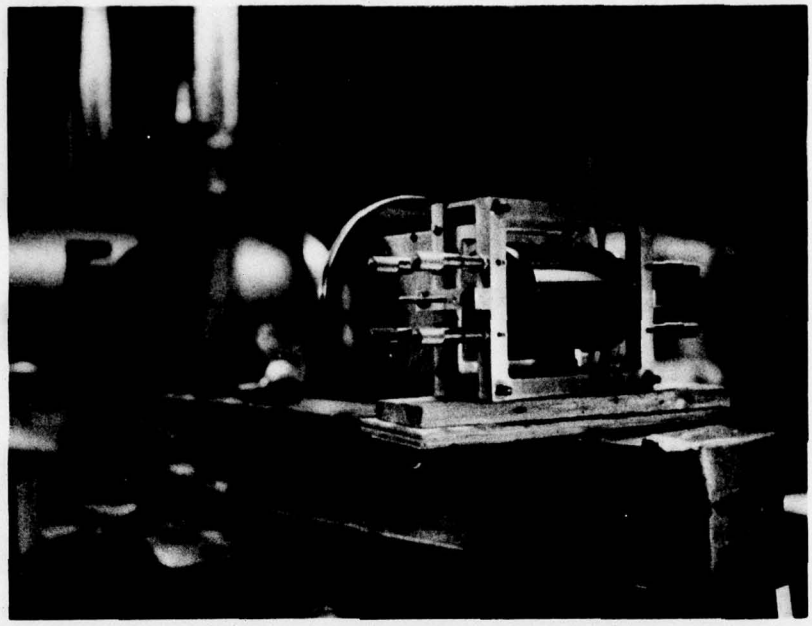

Fig. 1d Shock Holder - Entry Portion

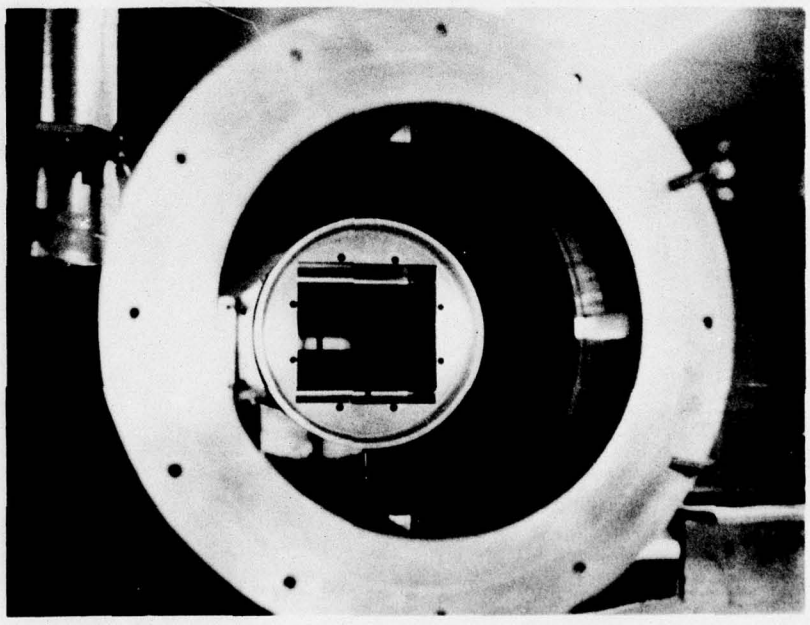

Fig. 1e Shock Holder - Throat Portion

Figure 1(Cont.) Major System Components.

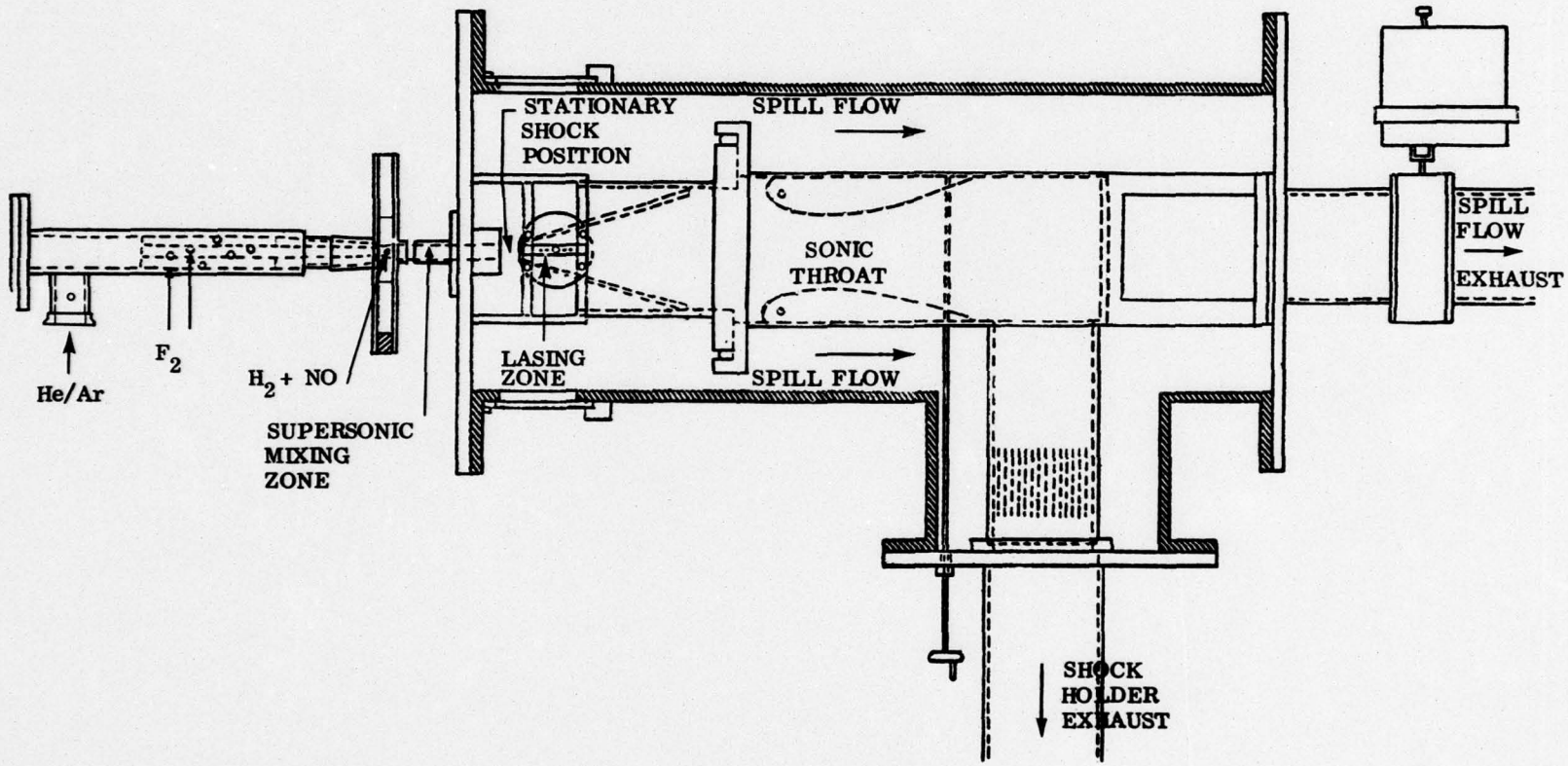

Fig. 1f System Assembly
Figure 1 (Cont.) Major System Components

at the inlet to the nozzle array. An upstream view of the plenum and conduit are shown in figure 1(b). The flange face shown is the inlet plane of the nozzle array and there the trailing edges of the core flow conduit are visible. Fluorine is injected through 11 holes equally spaced across the core flow in each of two tubes which traverse the plenum at positions approximately 30 cm upstream from the nozzle inlet plane. The shroud flow, which does not contain reactive gases, serves to isolate the walls of the supersonic-mixing region and the upstream portion of the shock holder and thereby prevent wall-induced reactions.

The 25 element nozzle array was fabricated from a single piece of berillium copper and is shown in an upstream view in figure 1(c). Two dimensional nozzle elements have a throat height of 1.27 mm with 4.06 mm spacing on centers and 0.25 mm trailing edge thickness. Converging nozzle walls are circular arcs and diverging walls are straight with a divergence half angle of 9.4^{o}. Secondary flow, consisting of hydrogen and nitric oxide, enters a manifold through four holes in the sides of the nozzle block. Secondary injection occurs through three slits along each trailing edge of the central 21 nozzle elements as is shown in three views of a single nozzle wall element in figure 1(c). Overall dimensions of the nozzle array are 2.0 cm in height and 10.0 cm width. Secondary injection is confined to the central 1.0 cm in height and 8.0 cm in width, which coincides with the fluorine-bearing core flow.

The supersonic mixing section, shown in figure 1(a), is rectangular in cross section and slightly divergent, increasing from 2.0 cm in height and 10.0 cm in width at the inlet to 3.05 cm in height and 11.2 cm in width over a length of 24.0 cm. The exit plane of the mixing section protrudes 2.54 cm into a cylindrical chamber (spill flow chamber) which is 38.0 cm in diameter.

The shock holder is shown in two elements in figures 1(d) and 1(c). The system assembly is shown in figure 1(f). Mirrors which are 10.0 cm in diameter form two walls of the shock holder inlet. One is concave spherical with a radius of curvation of 5.0m, the other is flat. Machined mirror edges from two sides of a sharp, rectangular entrance which is positioned 2.54 cm downstream from the exit of the supersonic mixing section. Copper plates form the other two walls and have a divergence half anlge of 11.8^{o}. This divergence prevents choking of the flow as the chemical reactions progress. Inlet width is 11.2 cm and the height is adjustable; settings of 2.51 cm and 2.11 cm were used for work reported here. The element in figure 1(d) mates to the element in figure 1(e) to convey the shock holder flow through cooling fins to a dump tank with a volume of 2.78 m^3. A sonic throat of variable height is shown in figures 1(e) and 1(f). External setting of this throat controls the position of the normal shock. In normal operation, flow is first established without reactions, then fluorine is introduced and the resultant reactions cause the flow to reestablish itself with the desired shock position. In the absence of reactions, the shock holder accepts the portion of flow appropriate to its inlet area with supersonic entry and attached external shocks. The sonic throat area is chosen so as to produce an internal shock pattern near the inlet. After the introduction of the final reactant, reactions proceed downstream from this shock pattern and the resultant rise in temperature prevents full flow acceptance by the fixed sonic throat. Consequently, the shock pattern is driven slightly upstream from the shock holder inlet, and it assumes a nearly normal configuration. The downstream subsonic flow diverges such that a portion spills over the inlet edges and the shock holder accepts only that portion of the flow which is consistent with the sonic throat area. High pressure

recovery and nearby stagnation temperature are achieved at the shock holder inlet and these conditions are appropriate to initiate the desired reactions for a chemical laser. The portion of flow which spills over the shock holder inlet exhausts to a separate dump tank with a volume of 5.57 m^3. This flow originates primarily from the shroud flow; consequently, it should experience little temperature rise due to reactions. The run duration for this blowdown system is controlled by spill flow. When pressure in the spill flow chamber exceeds the static pressure at the exit of the mixing section, it influences conditions at the shock holder inlet. At moderate overpressures the shock pattern enters the supersonic section and flow stability ceases.

III. FLUID FLOW INSTRUMENTATION AND CONTROL

Chemical composition is determined from flow rates of the various constituents through calibrated metering orifices. Pressures in supply reservoirs are recorded on a single channel of an oscillograph through a scanner which samples each of four pressure transducers at 0.05 sec intervals. These transducers are calibrated against a Heise Bourdon-tube gauge which has a calibrated accuracy of ± 10 torr over a pressure range of 0 to 10^4 torr. A schematic of flow-monitoring temperature and pressure instrumentation is shown in figure 2. Metering orifices are each calibrated by measuring the rate of decrease of pressure in a measured volume which exhausts to vacuum through the orifice. Four oscillograph channels continously record transducer measurements of: primary plenum pressure, static pressure at a station 0.635 cm upstream from the exit to the supersonic mixing section, stagnation pressure upstream from sonic throat, and stagnation pressure

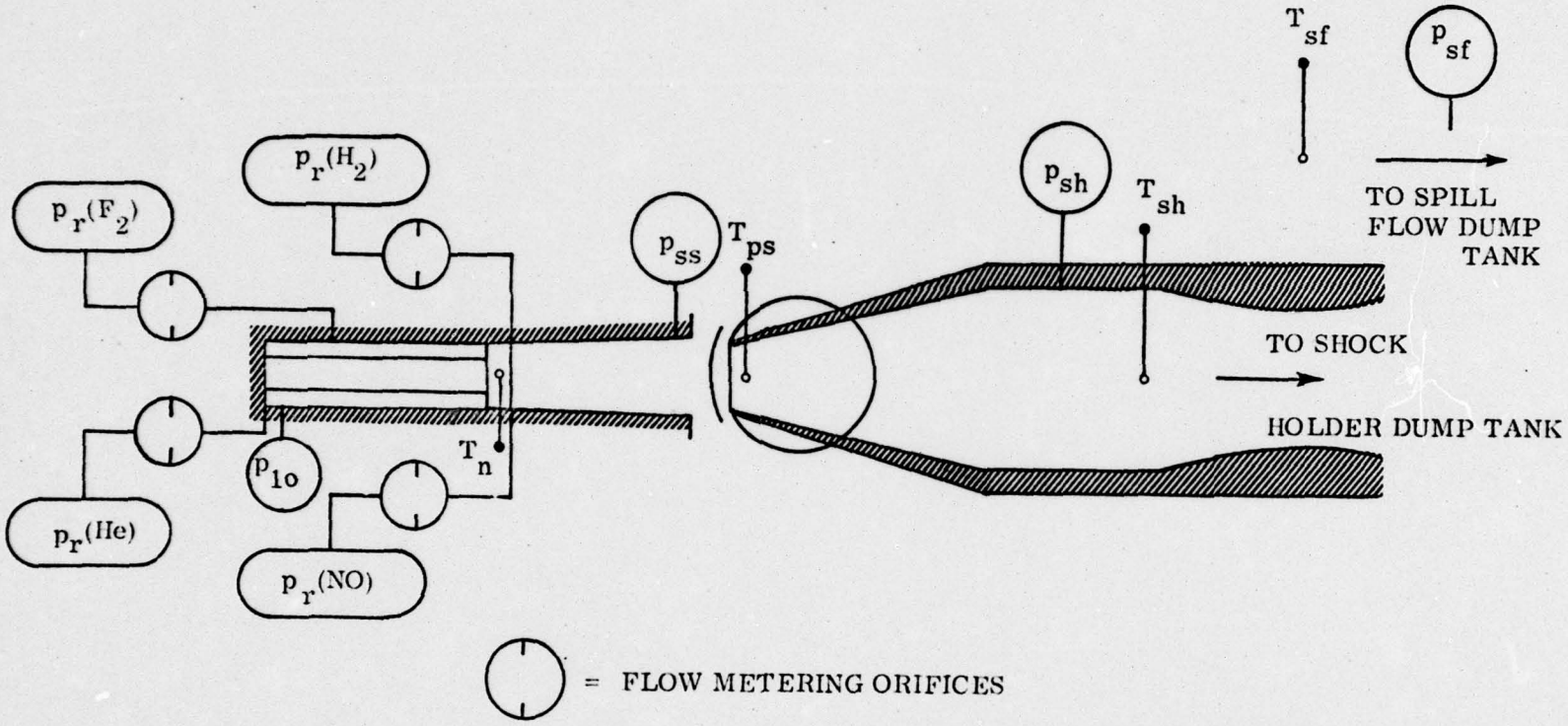

Figure 2 Flow Instrumentation Schematic

in the spill flow chamber. These data channels are calibrated against two MKS-Baratron capacitance pressure gauges with ranges of 0 to 10 torr and 0 to 1000 torr. Nozzle temperature is sensed with a Chromel/Alumel thermocouple. Gas temperature at stations 1.58 cm and 33 cm downstream from the shock holder inlet are sensed with Platinum/Platinum - 13% Rhodium thermocouples which are sheathed in Inconel (sheath outer diameter = 0.20 mm). These temperatures are recorded continuously on separate oscillograph channels. Spill flow temperature was not monitored regularly, since this thermocouple did not respond to a noticeable degree in its low pressure environment. The remaining four channels on a twelve channel oscillograph are dedicated to laser performance instrumentation discussed below.

Before each run, the dump tanks and test chamber are evacuated to a pressure below 0.2 torr and the dump tanks are isolated from the test chamber by electrically drive butterfly valves. Each gas reservoir is isolated from the system by a solinoid-controlled helium-driven ball valve. Valve and recorder operations are controlled by sequentially-triggered variable time-dealy relays.

Shock position and shape are observed with a Schieren system which views the region between the exit of the supersonic mixing section and the entrance to the shock holder. The system employs a xenon arc lamp, 48.4 mm focal length lenses, and a 16 mm motion picture camera which operates at 64 frames per second.

IV. LASER INSTRUMENTATION

Cavity mirrors, 10.0 cm in diameter and 6.35 mm thick, are instrumented with six chromel/alumel thermocouples which were imbedded beneath the outside surfaces with thermally conducting and electrically insulating epoxy, in a pattern shown in figure 3. A thermistor was attached to the reflecting face of each mirror in a region outside the shock holder as shown in figure 3. Five cavity-sampling holes, 0.76 mm in diameter, were drilled through the flat mirror as shown in figure 3. Cavity laser intensity is viewed by a 4.0 mm x 4.0 mm Pb/Se detector through a CaF_2 window and an IR quartz focusing lens. The focusing lens is positioned 30 cm from the center of the cavity and the detector is positioned at the lens focal length, 36.5 cm. The diffraction limited laser beam resolution of 10 mrad would indicate that the detector sees only a portion of the radiation emitted through each sampling hole.

Two positions of the cavity optical axis (i.e., position of co-normals of flat and spherical mirrors) were studied; one was coincident with the hole (b) of figure 3 and one was midway between holes (a) and (b) of figure 3. When referenced to the shock holder inlet these correspond to $x_c = 3.28$ cm and $x_c = 1.85$ cm, respectively. These positions allow precise mirror alignment and detector positioning with an He/Ne laser using the existing hole pattern. Mirror thermocouples are connected in series as pairs to yield a direct response of 80 $\mu v/^{o}C$. Each pair consists of one thermocouple from each mirror at the same stream-wise station. Four paired thermocouple data channels are recorded on a single oscillograph channel through a scanner with a sampling rate of 40 Hz. Thermistor signal is recorded during each run to provide a sensitive measurement of mirror temperature rise after the

With Respect to Inlet

x_a = 0.424 cm	x_1 = 1.54 cm	x_4 = 5.35 cm
x_b = 3.28 cm	x_2 = 2.81 cm	x_5 = 6.62 cm
x_d = 6.14 cm	x_3 = 4.08 cm	x_6 = 7.89 cm
x_e = 9.00 cm		

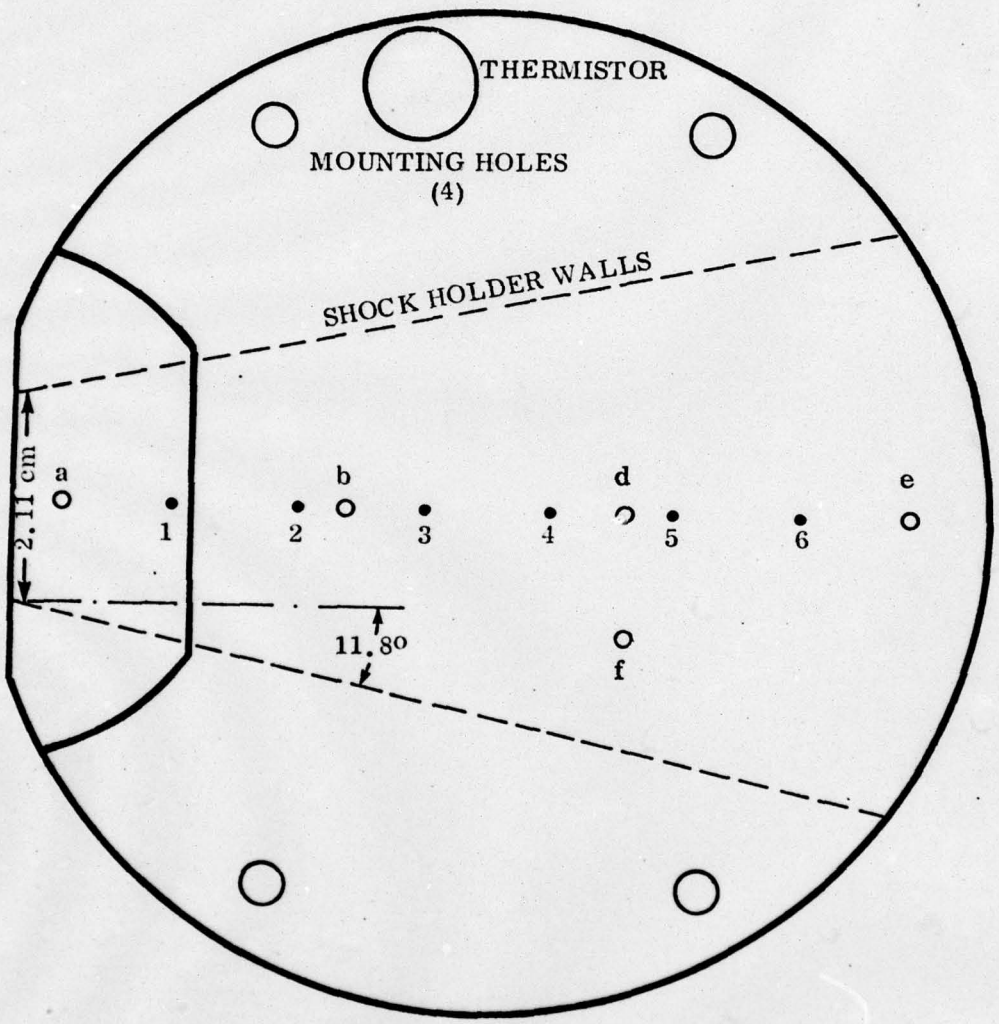

● Thermocouple Connections 1 through 6 Both Mirrors.

O Cavity Sampling Holes a through e (0.75 mm diam.) Flat Mirror

AL-1773

Figure 3 Laser Performance Instrumentation

achievement of temperature uniformity. With amplification the oscillograph response to mirror thermocouples is $0.58^{o}C$/cm and its response to thermistor is $0.072^{o}C$/cm.

A chopper disc placed between the system and the focusing lens allows the Pb/Se detector to sample sequentially and periodically the radiation from each of the holes, a - b - d - e (hole f was normally masked). The detector output is continuously displayed in two oscillograph channels with responses of 92 mw/cm and 1.83 mw/cm, respectively; where units refer to total power onto the detector per centimeter of recorder displacement. These detector channels are used as indicators of relative cavity power; the above responses are based upon supplier's calibration of detector responsivity.

V. FLOW MEASUREMENTS

A representative oscillograph trace is shown in figure 4 in which only significant flow measurements are included for present purposes. Laser instrumentation channels were not active and the nozzle temperature channel was masked. Figure 2 shows temperature and pressure notation. Channel 1 periodically records a timing mark followed by two scans through the four supply-gas reservoir transducers in the sequence p_r (F_2), p_r (H_2), p_r(Ar), p_r (NO). Timing marks are spaced at 0.1 sec intervals. This portion of the trace began just prior to Ar turn-on and ended just after F_2 turn-off; H_2 and NO turn-on occurred in earlier time and H_2, NO and Ar turn-off occurred in later time. The rise in primary plenum pressure p_{10} and supersonic static pressure to nearly constant levels in response to Ar turn-on shows that supersonic flow was properly established in the mixing section. The rise in

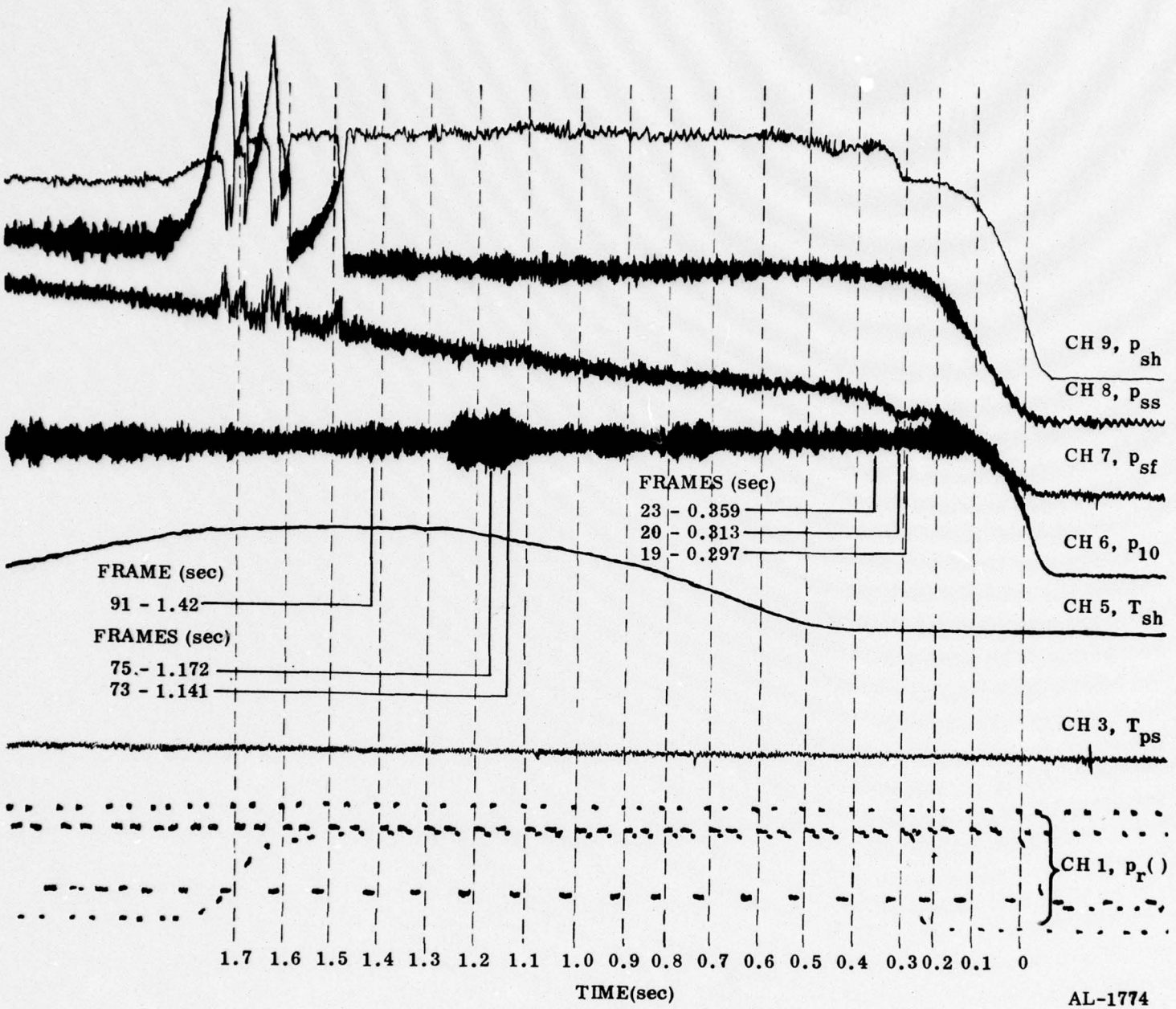

Figure 4 Oscillograph Trace for Flow Studies

side flow stagnation pressure, p_{sf}, and shock holder stagnation pressure, p_{sh}, to nearly constant values prior to F_2 turn-on shows the existence of steady flow in both regions; hence, the dump tank entry valve for spill flow was choked. There was no response in p_{10} or p_{ss} to F_2 turn-on which indicates that chemical reactions did not occur to a significant extent in the mixing region. Shock holder pressure rose abruptly to a nearly constant level in response to F_2 turn-on which suggests the occurrence of a new stationary shock pattern with a higher recovery pressure associated with shock positioning farther upstream. Spill flow pressure rose abruptly and continued to rise thereafter, which indicates an increase in spill flow in response to F_2 turn-on and almost coincidentally the end of choking at the tank inlet valve.

The point in figure 4 where p_{10} reached half its maximum value was chosen as the time origin. Calibrated values of pressure and temperature variations are given in Table I at three times: $t = 0.3$ sec, which corresponds to the first plateau in p_{sf} and p_{sh}; $t = 0.4$ sec, which is near the beginning of the second plateau in p_{sh}; and $t = 1.49$ sec, which corresponds to the termination of undisturbed flow in the supersonic mixing chamber. It is noted that temperatures recorded in Channels 3 and 5 (postshock temperature, T_{ps}, and shock holder temperature, T_{sh}, respectively) do not represent instantaneous gas temperature; response time in the recorded flow environment is the order of 1.5 sec. However, the temperature rise in Channel 5, ΔT_{sh}, clearly shows the occurrence of combustion in the shock holder. Channel 3, T_{ps}, records a Pt/Pt-13% Rh thermocouple with a gain setting of 0.498 mv/cm. This would show a detectable 1.0 mm deflection for 8.3°C temperature rise One thus concludes from Table I, that prereaction in the supersonic mixing section

consumed less than 1.2% of the fluorine which corresponds to a stagnation temperature rise of less than 8.3°C. Prereaction at this low level is expected to have small influence on laser performance.

Shock holder pressure recover, p_{sh}/p_{ss}, of 9.27 is reported in Table I. High pressure recovery is of considerable importance in practical laser application. If flow separation is assumed to occur at the shock holder inlet, it may be reasonable to assume that p_{sh} represents static pressure on the downstream side of a normal shock. Normal shock relations and p_{ss} then provide an estimate of Mach number at the mixing chamber exit as 2.45, and a static temperature of 98°K. Flow at this Mach number corresponds to an inviscid area ratio of 2.08; whereas, the geometrical ratio of mixing section exit plane area to nozzle array throat area is 5.28. This implies a fractional reduction in stagnation pressure of 0.363 due to boundary layers and mixing. Table I and figure 4 show that disturbances enter the supersonic mixing section when p_{sf} reaches a value near p_{ss}; thus, under these viscous conditions a jet can tolerate little or no overexpansion without flow separation at the nozzle walls.

Schlieren photographs were taken during the above run at a rate of 64 frames per second. Six frames are shown in figure 5 which serves to illustrate various features of the shock pattern history. The time origin was taken at the first appearance of a shock pattern in a stable form. This form, as shown in figure 5(a), persisted through frame 19. It then changed to a stable shock positioned upstream from the holder inlet as shown in frame 20, figure 5(b). Frame 23, figure 5(c) shows more clearly the concave shape of the shock which is presumably due to separated flow near the walls of the shock holder inlet. The shock remained stable in this form for

Certain Flow Temperature Variations and Pressures from figure 4:

F_2 - 0.0091 moles/sec NO - 0.0028 moles/sec

H_2 - 0.0096 moles/sec Ar - 0.81 moles/sec

X_{F_2} - 2.7% X_{H_2} - 2.9% X_{NO} - 0.87%

Reactive Core Flow is 40% of Total Flow

Shock Holder Inlet Height = 2.51 cm

Sonic Throat Area = 22.6 cm^2

Time (sec)	p_{10} (torr)	p_{ss} (torr)	p_{sh} (torr)	p_{sf} (torr)	ΔT_{ps} (^oC)	ΔT_{sh} (^oC)
0.3	136.5	3.13	23.9	1.88	0	0
0.4	136.5	3.13	29.0	2.46	0	0
1.49	127.4	3.21	29.0	3.43	0	312

Table I

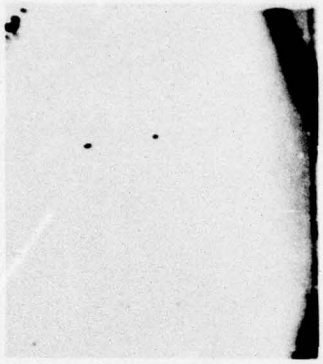

a

Frame 19

t = 0.297 sec

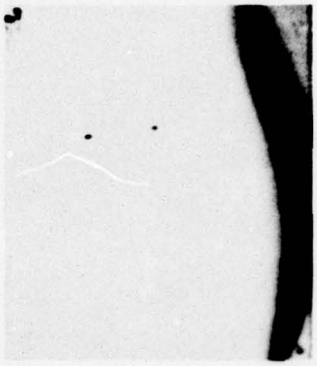

b

Frame 20

t = 0.313 sec

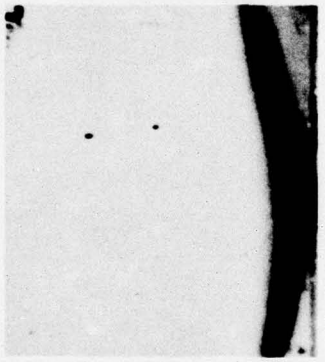

c

Frame 23

t = 0.359 sec

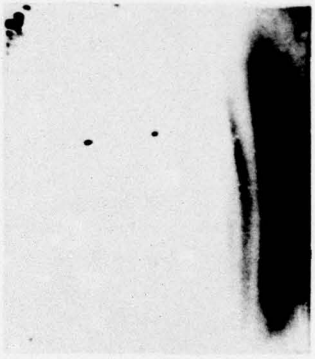

d

Frame 73

t = 1.41 sec

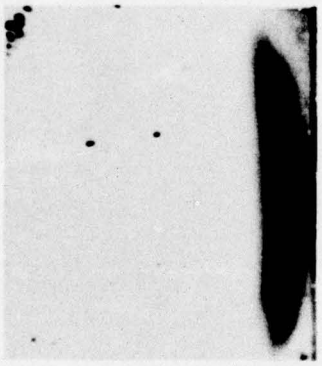

e

Frame 75

t = 1.172 sec

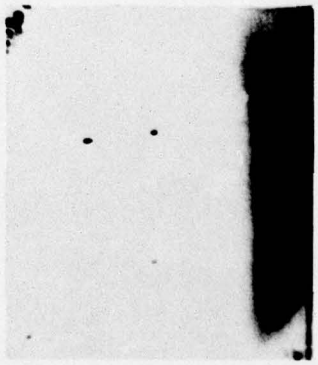

f

Frame 91

t = 1.423 sec

AL-1775

Figure 5 Schlieren Photographs at Times Keyed to Figure 4

most of the duration of undisturbed supersonic flow. However, it occassionally assumed as oscillatory form for periods of 3 or 4 frame as illustrated in figure 5(d), frame 73, followed by rapid recovery to the stable form of figure 5(c), frame 75. After frame 91, figure 5(f), the shock disappeared abruptly and reappeared only fleetingly many frames later. Times associated with the frames of figure 5 are shown in figure 4. Within the limits in timing accuracy in figures 4 and 5, the Schlieren observations completely support the description of flow history given above. Prior to F_2 turn-on the shock pattern was mainly within the shock holder; after F_2 turn-on, the shock was stable and was positioned upstream from the shock holder; at the time of onset of disturbances in the supersonic mixing section, the shock pattern left the field of view. The run presented here was more stable than others performed at lower values of p_{10}. Runs with helium as diluent provided Schlieren contrast barely sufficient to view shock history at plenum pressures above 100 torr. These helium runs showed a shock pattern similar to that of figure 5(d) which was predominately oscillatory over a stream-rise distance of approximately 1.0 cm. For the purposes of laser demonstration, this degree of oscillation was acceptable. To insure shock stand-off for a given set of flow conditions, sonic throat area was reduced continually during a set of runs and the selected operating area was that for which no further increase in p_{sh} and T_{sh} was observed.

VI. OPTICAL STUDIES OF LASER CAVITY INTENSITY

A lead-selenide detector sequentially viewed laser cavity intensity through four holes in the flat mirror. Manufacturer's calibration was used for data interpretation. A diffraction limited beam resolution of 10 mrad indicates that only a portion

of sampled beams reached the detector. Consequently, the measurements are qualitative in nature and likely underestimate cavity intensity. Mirror thermocouple channels were operational during the run presented here; however, their physical contact with the mirrors was questionable and thermal isolation of dissimilar-junction vacuum feed-throughs was not adequate. Therefore, mirror thermocouple measurements are discussed in Section VII which reports on measurements obtained after these problems were corrected. Spill flow dump-tank volume was 2.88 m^3 when measurements of this section were obtained; run time was extended by increasing the volume to 5.57 m^3 prior to measurements reported in Section VII.

A series of runs using both helium and argon as diluents were conducted with a mirror conormal station (optical axis) x_c = 3.28 cm, and with a shock holder inlet height of 2.51 cm. Results with argon diluent showed low level and intermittent laser radiation for a variety of plenum pressures, chemical compositions and sonic throat areas. During attempts to increase laser intensity there arose the suspicion that, with argon as diluent, x_c was too large in runs with high reactant concentrations; consequently, helium was used as diluent in the remaining studies. A series of runs were conducted with helium diluent for the purpose of increasing laser cavity intensity within limitations of the gas handling systems and with fixed optics (x_c = 3.28 cm). One representative run which corresponds to maximum observed cavity intensity is presented here. Since this run was selected from a very limited matrix of pressures, compositions and sonic throat areas, it is not perported to represent maximum attainable power for the present fixed laser optics. It does serve to demonstrate the achievement of laser power extraction from a

detonable gas mixture during a time interval which is very long compared to unsteady shock transit times. It further points to the possibility of achieving substantial laser power extraction in such a configuration.

The oscillograph trace for the selected run is shown in figure 6 and a summary of operating conditions and results are shown in Table II, where flow conditions refer to the time of peak laser intensity. The plenum transducer signal in Channel 6 typically showed very large oscillation for helium diluent runs; this may result from a flow resonance in the helium delivery tube or within the cavity of the transducer itself. Since these oscillations had no noticeable effect on supersonic flow conditions and since small scale flow disturbance might aid in the mixing process, no attempt was made to correct this condition. The postshock thermocouple probe, Channel 3, indicates cooling prior to lasing, heating during lasing, and cooling after lasing. Adiabatic cooling of the He supply reservoir offers a reasonable explanation of cooling and laser cavity radiation is likely the cause of heating; this is discussed further in the next section.

Cavity power incident in the Pb/Se detector was recorded in Channels 4 and 12. The chopper disc scans mirror holes in the sequence e - d - b - a. Channel 12 shows detectable power from holes a, b, and d, which is consistent with the optical axis being coincident with hole b. Peak detected power of 117 mw emanated from hole b at time 0.51 sec. This is determined from Channel 4 which has a sensitivity of 92 mw/cm. The corresponding detected power from each of holes a and d was 1.86 mw as determined from Channel 12 with a response of 1.83 mw/cm. If all laser radiation emitted from each hole reached the detector, the associated cavity intensities would be 51.4 w/cm^2 along the optical axis and 0.82 w/cm^2 at stations corresponding to holes a and d.

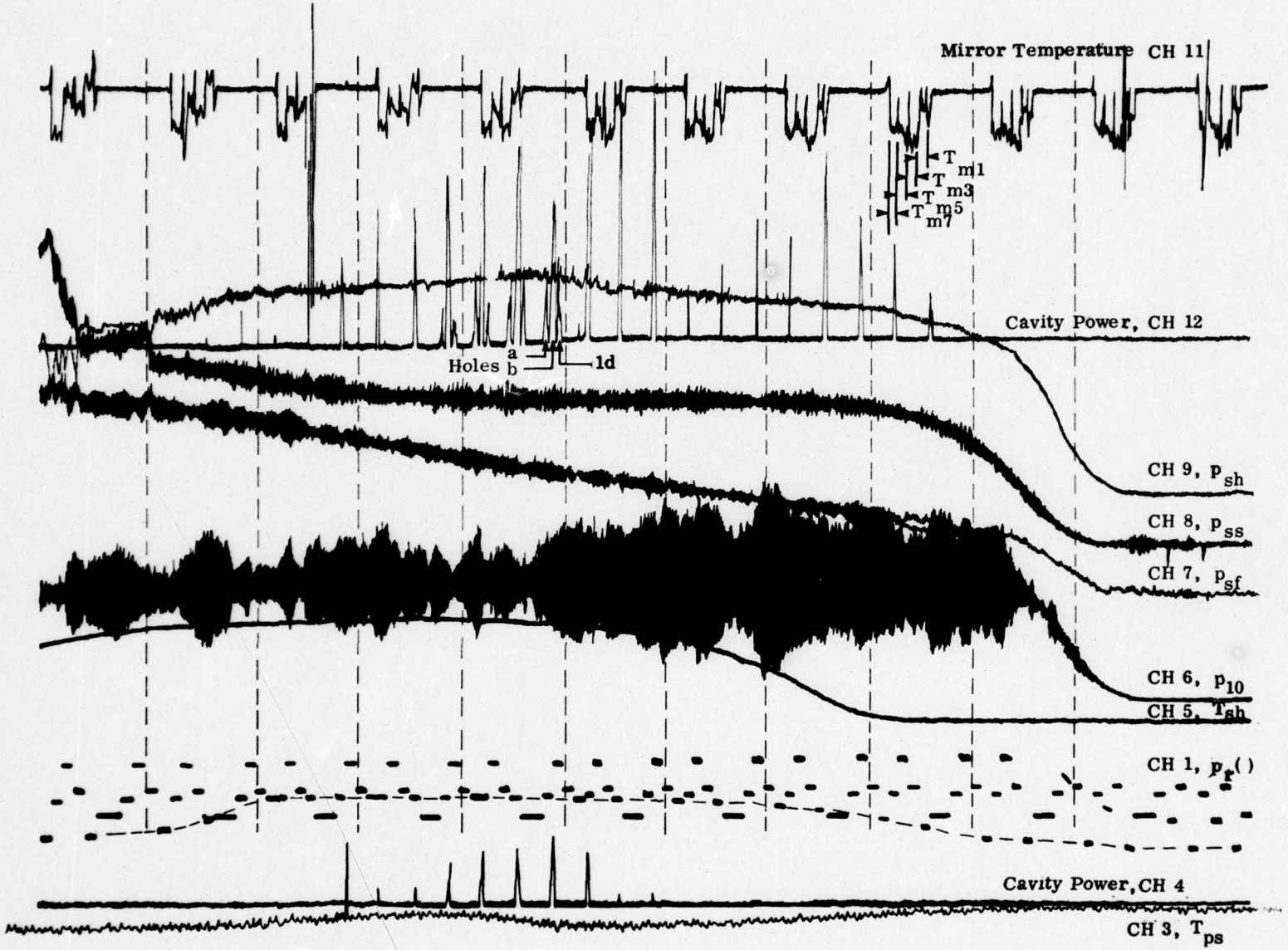

Figure 6 Observation of Cavity Radiation

Operating Conditions and Measurements Corresponding to the Run in figure 6:

F_2	-	0.035 moles/sec	NO	-	0.015 moles/sec
H_2	-	0.020 moles/sec	He	-	1.71 moles/sec
X_{F_2}	-	4.9%	X_{H_2} -	2.8%	X_{NO} - 0.84%

Shock Holder Inlet Height = 2.51 cm

Sonic Throat Area = 26.1 cm^2

Maximum Power Incident on the Pb-Se Detector (Hole b) = 117 mw

Peak Cavity Intensity if all Probe Beam is Captured = 51.4 w/cm^2

Simultaneous Incident Power from Each Adjacent Hole = 1.85 mw

Duration of Laser Operation = 0.16 sec

p_{10}	=	107 torr	p_{sf}	=	2.7 torr
p_{ss}	=	3.0 torr	ΔT_{ps}	=	$-4.2^{o}K \rightarrow 17^{o}C$
p_{sh}	=	25.7 torr	ΔT_{sh}	=	$333^{o}C$

Table II

Detected power from hole b remained above 70 mw for a duration of 0.16 sec during a stable flow time of 0.7 sec. The delay in laser initiation was presumably due to the slow rise F_2 pressure in the volume between flow orifice and injector. This slow pressure rise is shown in Channel 1 where the F_2 gate was transferred from the reservoir pressure transducers, p_r (F_2), to one located in the above volume, p_1 (F_2). A broken line is used to illustrate this gate response in figure 6. This F_2 gas handling feature was present in work reported in Sections VI and VII. Laser termination prior to steady flow termination was observed in most helium diluent runs. Although several plausible explanations for this occurrence may be offered, none were explored in detail in the present work.

VII. LASER POWER EXTRACTION BY MIRROR HEATING

A series of runs were conducted with He as diluent; the laser optical axis (conormal station) was positioned at x_c = 1.85 cm and the shock holder inlet height was 2.11 cm. Side-flow dump-tank volume had been increased to 5.57 m^3 which extended run times over those reported in Section VI. Mirror thermocouple contacts were secured by thermally conducting and electrically insulating epoxy. Dissimilar-junction vacuum feed-throughs were isolated from the chamber by silicone potting. Mirror thermocouple pairs, one on each mirror at a common stream-wise station were wired in series to provide an amplified oscillograph sensitivity of 0.58°C/cm in Channel 11. Thermocouple stations 1, 2, 3 and 6 were monitored; however, incorrect wiring of station 6 rendered it useless. Thermistors on either mirror were recorded in Channel 10 with a sensitivity of 0.072°C/cm. An oscillograph of one run is shown in figure 7 and the summarized results of two runs are shown in

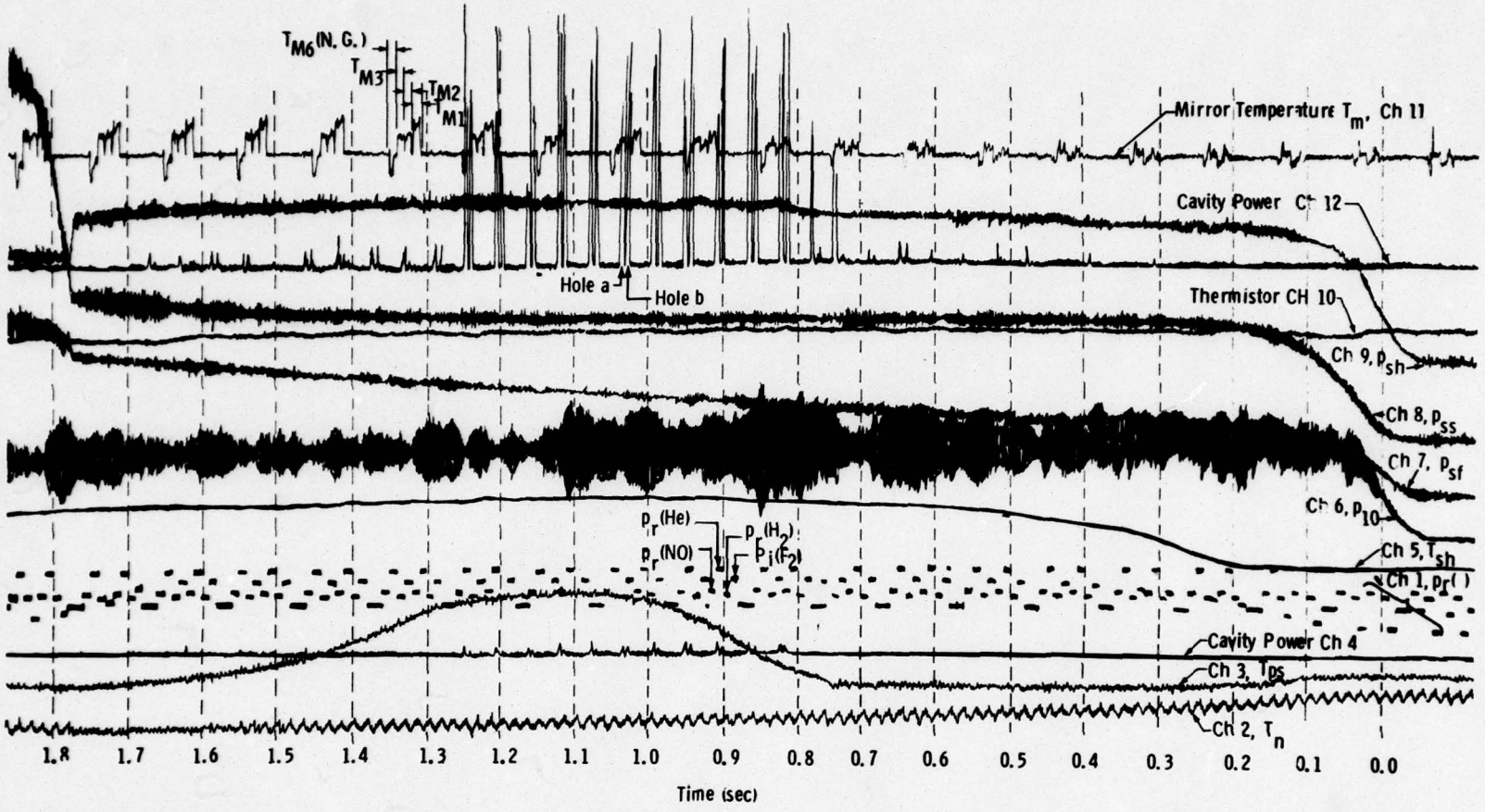

Figure 7 Observation of Laser Cavity Radiation and Mirror Heating - Run 6 of 2/1/77

Table III, where operating conditions refer to the time of peak cavity radiation. The only difference in operating conditions between these two runs was shock holder throat area.

Nearly steady flow was maintained for 1.78 sec, as shown in figure 7. Strong laser operation occurred from t = 0.7 sec to t = 1.3 sec. Delay in laser initiation may be due to the slow rise in p_i (F_2) as shown in Channel 1; however, initiation was abrupt and coincided with an abrupt though slight rise in shock holder pressure as seen in Channel 9. Laser termination occurred 0.3 sec before F_2 shut-off; whereas, flow conditions were nearly constant until F_2 shut-off. The drop in He pressure of 17% between flow start-up and laser termination suggests a possible drop in plenum stagnation temperature of 21°K, which might cause retarded F atom production leading to laser termination. However, this speculation is not supported by T_{ps} in Channel 3, which shows an initial adjustment to constant temperature after He turn-on and readjustment to that temperature after laser radiation heating terminates. The rise indicated in T_{ps} during laser operation can be explained adequately by the balance of strong irradiation at its station x = 1.58 cm, which is near the optical axis, and conduction cooling by the unreacted gas. Radiation cooling time for this thermocouple is of the order of 15 sec; consequently, responses in Channel 3 to abrupt laser initiation and termination represent fluid conduction time response.

Cavity radiation in data Channels 4 and 12, with respective sensitivities to detected power of 92 mw/cm and 1.83 w/cm, show measurable signals from holes a and b with peak power levels of 37 mw and 30 mw, respectively. These power levels do not relate to peak or average cavity intensity, since the optical axis was

Operating Conditions and Measurements for Runs 5 and 6 of 2/1/77:

F_2	= 0.037 moles/sec			NO	= 0.015 moles/sec
H_2	= 0.015 moles/sec			He	= 1.53 moles/sec
x_{F_2}	= 5.8%	d_{H_2}	= 2.3%	x_{NO}	= 2.3%

Primary plenum pressure p_{10}	= 110 torr
Supersonic *static* pressure p_{ss}	= 3.1 *torr*
Shock holder inlet height	= 2.11 cm
Optical Axis, x_c	= 1.85 cm
Total heat capacity of mirror pair	= 327j/^oC
Mirror heat capacity per unit area	= 2.18j/cm^2 ^oC
Mirror thermal response τ/x^2	= 0.214 sec/cm^2

		Run 5	Run 6
Shock holder throat area (cm^2)		26.1	24.0
Peak post shock thermocouple rise ΔT_{ps}(^oC)		100	146
Peak shock holder temperature rise ΔT_{sh}(^oC)		291	305
Shock holder pressure (torr)		22.9	24.4
Shock holder capture (%)		70	68
Duration of laser operation (sec)		0.7	0.6
Local laser power extraction, each mirror (w/cm^2), based on local temperature rise	Station x_1	1.25	1.27
	Station x_2	0.72	1.02
	Station x_3	0.53	0.51
Total energy to mirror based on steady state temperature rise (joules)		65	75
Estimated laser outcoupled power based on local mirror heating = 20 watts	Chemical efficiency = 0.25%		

Table III

midway between these holes. Still, the inferred local cavity intensities of 16 w/cm^2 and 13 w/cm^2 at the fringes of the lasing region suggest substantial cavity radiation.

The fraction of total flow which was captured by the shock holder is determined iteratively using known total flow rate, core flow composition, shock holder stagnation pressure and temperature, and shock holder throat area. Iteration is required, since the average molecular weight of shock holder flow depends upon capture fraction. Values for Runs 5 and 6 are shown in Table III as 0.70 and 0.68, respectively. For comparison, the geometrical capture fraction, i.e., the ratio of shock holder inlet area to mixing section exit area, was 0.69. An independent estimate of capture was carried out for Case 6 in which the rate of rise in spill flow pressure, p_{sf}, and spill flow dump tank volume were used to determine spill flow rate. It was assumed that the dump tank pressure was equal to p_{sf} and that filling occurred at constant temperature. Both of these assumptions would tend to overestimate spill flow fraction; however, the result shows:

Spill Flow Fraction	Capture Fraction
$(1-f) = 0.295$	$f = 0.68$

$$(1-f) + f = 0.975$$

This result is somewhat fortuitous, since this consistency exceeds pressure measurement accuracy ($\pm 4\%$). In a similar way, the calibrated flow rates of F_2 He in Run 6 were related to measured primary plenum pressure and ambient temperature to provide a calculation of total effective area for the primary nozzle throat of 5.03 cm^2. Comparison with the geometrical primary throat area of 6.45 cm^2 indicates a reduction of 22% due to viscous effects.

If one assumes that all reactive flow enters the shock holder, then stagnation temperature rise due to chemistry may be calculated from capture fraction, initial mole fraction of H_2, and the heat of formation of 2 HF, h_f, as

$$\Delta T_{sh} = 0.4\, f^{-1}\, h_f\, c_p^{-1}\, x_{H_2}$$

For Runs 5 and 6 this yields $\Delta T_{sh} = 343^{o}K$ and $353^{o}K$, respectively, where h_f = 133.5 kcal/mole and $c_p = 5.12$ cal/mole^{o}K. These calculations are in agreement to within 17% of measurements reported in Table III.

Local mirror heating during laser operation was determined from the scanned thermocouple display in Channel 11 as shown in figure 7. Examination of each of three channels in figure 7 shows that T_{m1}, T_{m2}, and T_{m3} rose measurably ($0.35^{o}K$, $0.28^{o}K$ and $0.14^{o}K$, respectively) during 0.6 seconds of laser operation and each shows no additional rise during 0.3 sec between laser termination and F_2 shut-off. Several observations of this pattern of events provide persuasive evidence that local mirror heating during laser operation is due to outcoupled power. Heat transfer calculations which ignore conduction in directions normal to mirror surfaces provide very conservative estimates of outcoupled power on the basis of these local temperature measurements. These are shown in Table III. A coarse description of lateral mirror heat transfer during 0.6 sec of laser operation provides a conservative estimate of average total outcoupled power for runs of Table III as 20 watts, which corresponds to a chemical efficiency of 0.25%.

The fourth mirror thermocouple channel was tied to thermocouple station 6 near the downstream end of the mirrors. Internal wiring errors caused this channel

to be inoperable; consequently, no local heating measurements outside the lasing region are presented. Subsequent runs, where this malfunction was corrected, showed that conduction heating in this region was comparable to outcoupled heating in the lasing zone. However, this heating was continuous during steady flow operation and showed no change related to laser operation. This conduction heating is likely due to flow separation. Both thermistors and mirror thermocouples provide a measure of final steady state temperature rise. These four redundant temperature measurements were typically in agreement to within ±15% after a period of 30 sec from the start of a run. The present rigidity of the experimental apparatus has not allowed the separation of conduction heating from laser heating in these steady state temperature measurements. These results are, none the less, presented in Table III as 65 and 75 joules for Runs 5 and 6, respectively. A system modification to allow remote adjustment of optical axis, x_c, would allow the isolation of these heating phenomena and, thus, provide a proper calorometric measurement of average laser outcoupled power.

VIII. SUMMARY

A continuously flowing detonable mixture of F_2, H_2, NO and diluent has been achieved at low temperature without significant reactions. Secondary injection of H_2+ NO along trailing edges of a nozzle array, into a cold supersonic stream containing F_2 plus diluent, was followed by diffusive mixing in a supersonic channel. A stationary shock wave was maintained in the stream after homogeneous mixing, which initiated steady state combustion. The present shock holder captured $\simeq 70\%$ of the total flow at a ratio of recovery pressure to supersonic static pressure in excess of 7.8. Laser

outcoupled power was achieved downstream from the stationary shock as determined from infrared optical measurements and from mirror heating. This is the first reported demonstration of CW laser operation in this configuration. Detected infrared laser power of 117 mw was obtained in a geometry for which chemiluminescent cavity radiation would be less than 4 μw. Mirror heating measurements provide a conservative estimate of time-averaged total outcoupled power in excess of 20w which corresponds to a chemical efficiency of at least 0.25%.

IX. ACKNOWLEDGMENTS

The author gratefully acknowledges assistance in chemical aspects of this work and in optical instrumentation and analysis from Morton Camac and Charles Kolb of Aerodyne Research, Inc. They are credited with the concept of combining NO initiation of the HF chain reaction with the stationary shock laser concept. The author is also grateful for design and computational assistance from Edward Powers and for design and fabrication work done by Henry Murphy.

The author is grateful for advice and guidance based upon years of related experience from several individuals and organizations which include: R. Limpaecher (AVCO-Everett Research Labs), T. Jacobs (TRW Systems), R. Oglukian and G. Canavan (DARPA), L. Wilson (AFWL) and W. Solomon (Bell Aerospace).

The author expresses special appreciation for assistance from the contract monitor Joseph Stregack of the Naval Research Laboratory and for advice and assistance in several areas from H. Mirels and members of the staff of the Aerospace Corporation.

REFERENCES

Adams, W.D., Turner, E.B., Holt, J.F., Sutton, D.G., and Mirels, H., "The RESALE Chemical Laser Computer Program (U)," Space & Missile Systems Organization Report No. SAMSO-TR-75-60 (20 February 1975)

Bowen, J.R., and Overholser, K.A., "An Appraisal of the Continuous Explosion Laser," J. Astron. Acta., Vol. 14, pp. 475-486, (September, 1967)

Cohen, N., and Bott, J.F., "A Review of Rate Coefficients in the H_2-F_2 Chemical Laser System," Space & Missile Systems Organization Report No. SAMSO-TR-76-82 (15 April 1976)

Cool, T.A., Stephens, R., and Shirley, J.A., "HCl, HF, and DF Partially Inverted CW Chemical Lasers", J. Appl. Phys., Vol. 41, pp. 10 (September, 1970)

Gross, R.A., "Design Report, Supersonic Combustion Tunnel," Air Force Office of Scientific Research Report No. AFOSR-TN-57-677 (September, 1960)

Gross, R.W.F., Giedt, R.R., and Jacobs, T.A., "Stimulated Emission Behind Overdriven Detonation Waves in F_2O - H_2 Mixtures," J. Chem. Phys. Vol. 51, No. 3, 1250 (August 1969)

Kolb, C.E., "Resonance Fluorescence Study of the Gas Phase Reaction Rate of Nitric Oxide with Molecular Fluorine," J. Chem. Phys., Vol. 64, pp. 3087 (April 1976) – also appears here as Appendix

Kolb, C.E., and Kaufman, F., private communication (1976)

Nicholls, J.A., Dabora, E.K., Gealer, R.L., "Studies in Connection with Stabilized Gaseous Detonation Waves," Seventh Symposium on Combustion, London, England (September, 1958)

Nicholls, J.A., Dabora, E.K., "Recent Results on Standing Detonation Waves," Eighth Symposium on Combustion, Pasadena, CA., (September 1960)

Nicholls, J.A., "Standing Detonation Waves," Ninth Symposium on Combustion, Ithaca, N.Y., (September 1962)

Richmond, J.K., and Shreeve, R.P., "Wind-Tunnel Measurements of Ignition Delay Using Shock-Induced Combustion," AIAA J., Vol. 5, p.1717 (October, 1967)

Suttrop, F., "Experiments Investigating Shock-Induced Combustion for Applications in Hypersonic Propulsion Engines," VI Europaischer Luftfahrt Kongress, Munchen, Germany (September 1965)

APPENDIX

RESONANCE FLUORESCENCE STUDY OF THE GAS PHASE REACTION RATE OF NITRIC OXIDE WITH MOLECULAR FLUORINE

C.E. Kolb

Aerodyne Research, Inc.
Bedford Research Park
Crosby Dr., Bedford, MA. 01730

(Received 22 December 1975)

ABSTRACT

Resonant fluorescent scattering of UV light absorbed by the 0,0 transition of the nitric oxide γ band at 226 nm was used to detect the decrease in NO concentration due to reaction with F_2 in a standard flow tube geometry. Rate measurements were performed under pseudo-first order conditions with F_2 in excess at temperatures between 168 and 359°K. These measurements yielded a temperature dependent bimolecular rate constant for the reaction of NO with F_2 of 7.0×10^{-13} exp (- 1150/T) with an estimated accuracy of ± 30%.

INTRODUCTION

The bimolecular gas phase reaction between nitric oxide and molecular fluorine:

$$NO + F_2 \xrightarrow{k_1} FNO + F \qquad (1)$$

has recently assumed technological importance due to its use as a purely chemical initiator for DF - CO_2 transfer chemical lasers[1-4] and H_2/F_2 chemical lasers.[5] In addition, Reaction 1 has been used as a source of F atoms in a number of kinetic studies.[6-8]

Relatively little work has been published on the kinetics of Reaction 1. Rapp and Johnston have reported a rate constant of 1×10^{-12} exp (-750 500/T) cm^3/sec based on studies of a dilute nitric oxide/fluorine diffusion flame operated at 195 and 300°K.[9] The rate data in this study were obtained somewhat indirectly from reaction profiles derived from visible flame chemiluminescence due to the radiative combination of F atoms with NO:

$$F + NO \longrightarrow FNO + h\nu \quad . \qquad (2)$$

More recently, Kim and co-workers have reported an average value for k_1 at 325 ± 10°K of $9.0 \pm 2.0 \times 10^{-15}$ cm^3/sec based on initial slopes of F atom production for an F_2/NO mixture in a flow tube with ESR detection of atomic fluorine.[7]

In addition to these studies, ratios of k_1 to the three-body recombination rate constant for F atoms with NO:

$$F + NO + M \xrightarrow{k_3} FNO + M \qquad (3)$$

have been reported by Hoell et al.[10] and Shirley et al.[11] However, even with recently determined values of k_3 now available[7,8] these measurements involve a number of kinetic assumptions and yield little direct information on k_1.

The order of magnitude difference between near room temperature values of k_1 from Refs. (7) and (9) illustrates the need for further kinetic studies of Reaction 1. The experiment described below is the most direct determination of k_1 reported to date. Measurement of NO consumption via Reaction 1 was monitored under controlled flow conditions by detection of resonantly scattered UV photons absorbed by the 0,0 transition of the NO γ bands at 226 nm. Care was taken to choose experimental conditions insuring the consumption of NO was due to Reaction 1 with little or no contribution due to Reaction 3.

EXPERIMENTAL

The flow reactor illustrated in Fig. 1 consisted of a 1m long, 2.54 cm diameter copper tube followed by a short stainless steel scattering cell containing apertures to two orthogonal 2.54 cm diameter, 15 cm long side arms with quartz end windows. Each windowed side arm aperture was opposed by an aperture leading into a short cylindrical light trap. An additional 20 cm length of copper flow tube downstream from the scattering cell connected the flow tube to a pyrex vacuum trap containing activated charcoal which served to convert F_2 and FNO to CF_4 prior to contact with vacuum pump oil. A one inch ball valve downstream of the charcoal trap was used to reduce pumping speeds and control flow velocities. A pair of Alcatel ZT 1060C vacuum pumps provided experimental flow speeds through the charcoal trap between 1 and 10 m/sec with total flow tube pressures between 1 and 4 torr.

F_2 diluted with N_2 was introduced at the upstream end of the 1m reactor section while NO was introduced through a radial disc at the end of a movable 0.6 cm stainless steel injector tube. A small He flow was introduced into the scattering cell side arms to protect the windows from F_2.

Three separate sections of 0.6 cm diameter copper tubing coiled were around the outside of the flow tube to allow the circulation of hot or cold liquids. This arrangement provided a means of regulating the reactor temperature between 77 and 360°K with a drift of less than 3° over the length of the flow tube and the duration of a rate measurement. Temperatures were measured with several copper-constantan thermocouples attached to the flow tube wall. Thin walled stainless steel sections of flow tube thermally isolated the variable temperature region from the movable injector O-ring seal, the glass vacuum trap and the windows of the scattering cell. Styrofoam insulation was fitted over the variable temperature region to aid in temperature stabilization.

Pressure taps in the flow section were connected to a halocarbon oil manometer to allow direct pressure measurements of the F_2 containing reaction mixture. The oil manometer was periodically calibrated with N_2 against a precision McLoed gauge.

Gases used in the rate experiments included CP grade NO (99% purity), ultrahigh purity He (99.999% purity) and an F_2/N_2 mixture all supplied by Matheson and used without further purification. The N_2/F_2 mixture was mass spectrometrically analyzed at an independent analytical laboratory as 96.3% N_2 and 3.7% F_2.

Gas flows were metered by stainless needle valves. The main N_2/F_2 flow rate was monitored with Matheson rotometers designed for fluorine applications. The rotometers were recalibrated after every other rate determination by determining the time required for a measured pressure rise in the known flow tube volume. The combined He and NO flows were always less than 3% of the N_2/F_2 flow. The flow tube was thoroughly passivated with molecular fluorine before use to avoid loss of F_2 due to wall reactions.

The relative NO concentration was monitored using the resonant fluorescence optical train illustrated in Fig. 2. Continuum UV light from a Varian 500 watt Xenon arc (model X6241-UV) was chopped and partially focused on a pin hole aperture. Light from this aperture source was focused through an iris, suprasil window, and flow tube side arm onto the center point of the flow tube. Light scattered at right angles to the input beam and flow direction was detected by a modified S-5 surface photomultiplier (EMI 9783B). A long wave cutoff filter supplied by Ditric Optics was inserted between the output window and the photomultiplier to remove visible and very near UV light scattered by nonresonant processes. The shortwave bandpass of the cutoff filter was designed to pass the 0,0 through 0,4 transitions of the NO γ system, all of which radiate substantially when the 0,0 transition is pumped. The output of the arc lamp fell off sharply below 226 nm so that negligible light was available to pump excited vibrational states of the NO A-state. The output signal from the photomultiplier was preamplified and read out on an PAR HR-8 lock-in amplifier which was referenced with the signal from an Electroproducts magnetic pick-up on the chopper assembly. Minimum detectable NO concentration (S/N = 1) with the resonance fluorescence setup was approximately 3×10^{13} per cm^3.

RESULTS

Experimental rate data were taken at five temperature groupings between 359 and 168°K. Data for two initial NO inputs were gathered for each F_2/N_2 input flow and flow speed setting. F_2 concentrations were calculated from oil manometer readings of the F_2/N_2 pressure, thermocouple flow tube temperature readings and the analyzed N_2/F_2 ratio. Flow speeds were determined in the usual manner from calibrated rotometer readings and total pressure measurements.

Sufficient reaction time was allowed to reduce the initial NO scattered UV signal, I^o_{NO}, measured with the NO injector ring 1.12 cm from the center of the scattering cell by at least 1/e. Figure 3 illustrates two examples of the measured decay of I_{NO} with increases in reaction distance. The linear I_{NO} semilog decay plot illustrates the validity of the pseudo first order kinetics $\left([F_2] >> [NO]\right)$ used to obtain rate constant values. No decay of the I^o_{NO} signal was observed as a function of NO injector position if the F_2/N_2 mixture was replaced with pure N_2. Experimental temperatures were chosen so that Reaction 1 would dominate NO consumption without serious competition from Reaction 3.

Table I contains experimental conditions for 22 seperate rate determinations and the resulting rate constants determined from I_{NO} decay plots similar to those in Fig. 3. A nonlinear least squares fit of the 22 rate determinations listed in Table 4 yielded an Arrhenius rate constant expression of:

$$k_1 = 7.04 \times 10^{-13} \exp(-1150/T) \qquad (4)$$

where T is expressed in °K.

DISCUSSION

By fixing the preexponential term in Eq. (4), the standard deviation of the 22 rate constant determinations listed in Table I from the fitted rate constant expression was obtained. The resulting exponential temperature dependence was - (1150 ± 41/T) indicating that the activation energy for Reaction 1 is 2.3 ± 0.1 kcal/mole. This value is consistent with the more indirectly determined value of 1.5 ± 1.0 kcal/mole of Rapp and Johnston.[9]

An analysis of possible systematic errors in F_2/N_2 flow rate determinations and oil manometer pressure readings was performed. The addition of probable systematic errors to the statistical uncertainty indicates that the accuracy of the rate constant expression (Eq. (4)) determined in this study is probably ± 30% over the experimental temperature range.

A plot of log k_1 versus 1/T plot for the 22 rate determinations listed in Table I is displayed in Fig. 4 along with a solid line representing Eq. (4). Figure 4 also contains the published rate data of Rapp and Johnston[9] and Kim et al.[7] As evidenced by Fig. 4 the near room temperature rate constant determined in this study is roughly a factor of two above that of Kim et al., and a factor of 5 below that of Rapp and Johnston. However, considering the indirect nature of Rapp and Johnston's diffusion flame measurements, and the need to rely on an initial slope analysis for the measurements reported in Ref. (7) the agreement with these studies is satisfactory.

The experimentally determined preexponential factor of 7.0×10^{-13} for the F_2/NO reaction is also in very good agreement with the value of 9.3×10^{-13} calculated by Herschbach[12] from the expected entropy of activation for Reaction 1.[13]

ACKNOWLEDGMENTS

The author would like to thank a number of colleagues at Aerodyne Research, Inc. for their help during the course of this study. In particular, he would like to acknowledge M. Camac, D. Mann, C. Gozewski, and E. Powers for their aid in experimental design and acquisition of components and R. Brown for valuable help in performing experimental measurements.

This research was sponsored by the Defense Advanced Research Agency through the Office of Naval Research, under Contract No. 00014-75-C-1123, and was monitored by the Naval Research Laboratory.

REFERENCES

1. T.A. Cool and R.R. Stephens, J. Chem. Phys. 51, 5175 (1969).
2. T.A. Cool and R.R. Stephens, App. Phys. Lett. 16, 55 (1970).
3. T.A. Cool, J.A. Shirley, and R.R. Stephens, App. Phys. Lett. 17, 278 (1970).
4. G.W. Tregay, M.G. Drexhage, L.M. Wood, and S.J. Andrysiak, IEEE J. Quant. Elec. 11, 672 (1975).
5. T.A. Cool, R.R. Stephens, and J.A. Shirley, J. App. Phys. 41, 4033 (1970).
6. T.L. Pollock and W.E. Jones, Can. J. Chem. 51, 2041 (1973).
7. P. Kim, D.I. MacLean, and W.G. Valence, NTIS AD 751456, (1972) and D.I. MacLean, private communication (1975).
8. C. Zetzsch, European Symposium of the Combustion Institute (ed. F.S. Weinberg) Academic Press, London, 35 (1973).
9. D. Rapp and H.S. Johnston, J. Chem. Phys. 33, 695 (1960).
10. J.M. Hoell, Jr., F. Allario, O. Jarett, Jr., and R.K. Seals, Jr., J. Chem. Phys. 58, 2896 (1973).
11. J.A. Shirley, R.N. Siles, R.R. Stephens, and T.A. Cool, American Institute of Aeronautics and Astronautics, paper 71 - 27 (1971).
12. D.R. Herschbach, M.S. Thesis, Standford University (1956).
13. D.R. Herschbach, H.S. Johnston, K.S. Pitzer, and R.E. Powell, J. Chem. Phys. 25, 736 (1956).

Table 1. Kinetic data for Reaction 1 as a function of flow temperature and other reaction conditions

Run Number	Temperature (^{o}K)	$F_2 \times 10^{-15}$ (cm^{-3})	I^{o}_{NO} (UV)	Flow Speed (m/sec)	k (cm^3/sec)
1	359	2.21	17.0	705	3.63×10^{-14}
2	359	2.21	25.0	705	3.08×10^{-14}
3	359	3.18	23.5	489	2.35×10^{-14}
4	359	3.18	16.3	489	2.70×10^{-14}
5	300	3.99	19.7	412	1.78×10^{-14}
6	300	3.99	17.5	412	1.72×10^{-14}
7	299	2.73	15.5	603	1.84×10^{-14}
8	299	2.73	20.0	603	1.76×10^{-14}
9	276	4.14	22.0	355	9.96×10^{-15}
10	276	4.14	15.5	355	9.40×10^{-15}
11	276	3.15	15.3	448	1.02×10^{-14}
12	276	3.15	24.5	448	8.97×10^{-15}
13	276	4.77	24.5	295	9.23×10^{-15}
14	276	4.77	19.2	295	9.00×10^{-15}
15	218	2.56	15.5	235	3.76×10^{-15}
16	217	2.59	22.0	234	4.12×10^{-15}
17	216	4.02	23.0	367	3.45×10^{-15}
18	215	4.04	15.2	365	3.04×10^{-15}

Table 1 (Cont.)

Run Number	Temperature (°K)	$F_2 \times 10^{-15}$ (cm^{-3})	I^o_{NO} (UV)	Flow Speed (m/sec)	k (cm^3/sec)
19	169	5.00	14.5	312	8.01×10^{-16}
20	169	5.00	17.7	312	7.03×10^{-16}
21	169	7.92	16.6	196	7.57×10^{-16}
22	168	7.92	13.6	196	8.77×10^{-16}

Figure Captions

Figure 1 Schematic of flow apparatus.

Figure 2 Schematic of nitric oxcide resonance fluorescence detection system.

Figure 3 Typical NO fluorescence decay curves versus reaction distance normalized to the NO fluorescence signal for an NO injector to scattering cell center distance of 1.12 cm. Straight line semilog decay plot indicates validity of pseudo first order kinetic treatment. Data represents runs 5 and 6 of Table 1.

Figure 4 This figure presents the available data for Reaction 1. The solid circles are a semilog plots of experimental rate constants versus 1/T for the kinetic runs listed in Table 1. The solid triangles are the data of Rapp and Johnston (Ref. (9)), while the open circles are the data of Kim et al. (Ref. (7)). The solid line is the best least squares fit to the data in Table 1, representing an Arrhenius rate constant expression of 7.0×10^{-13} exp (- 1150/T) cm^3/sec.

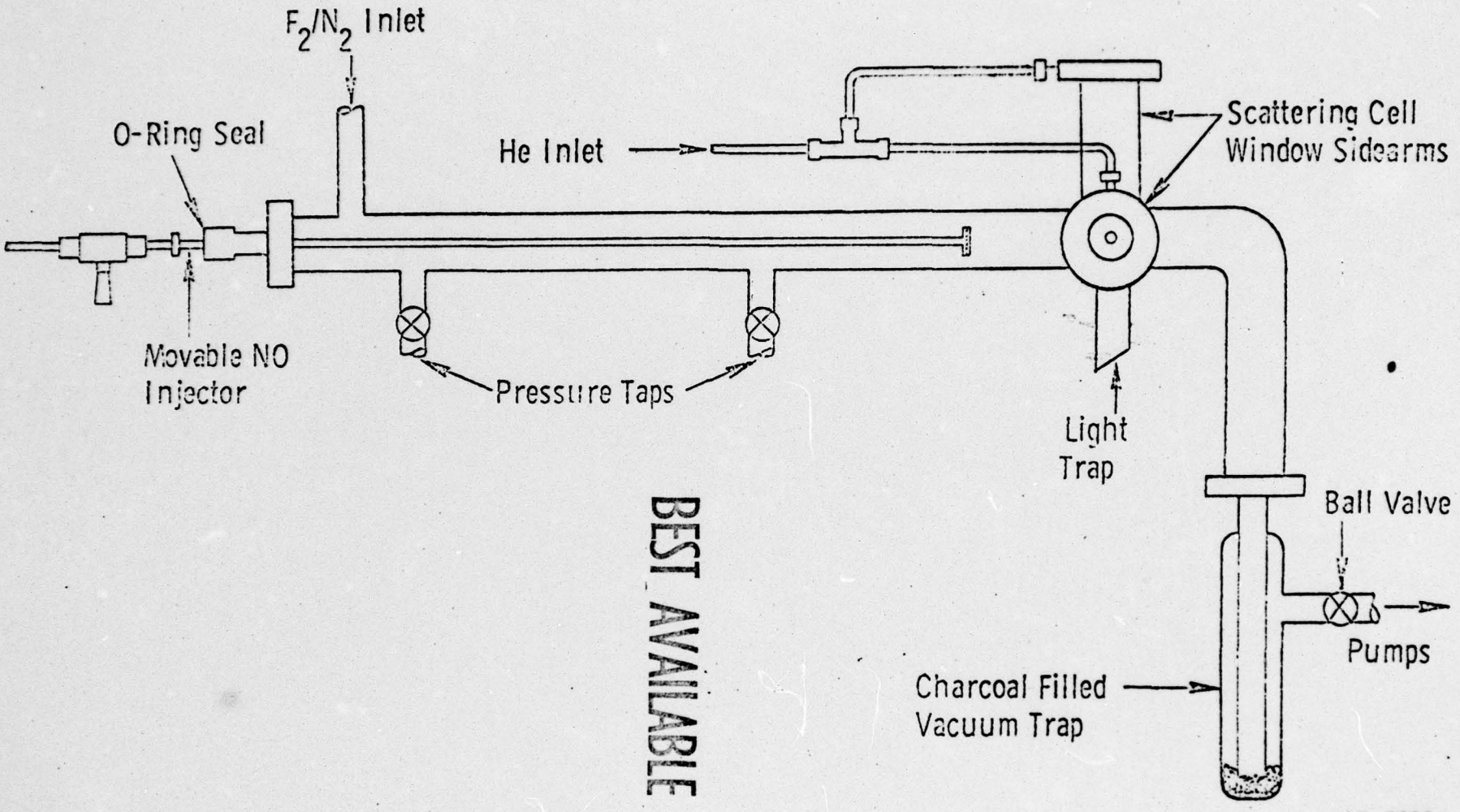

Figure 1

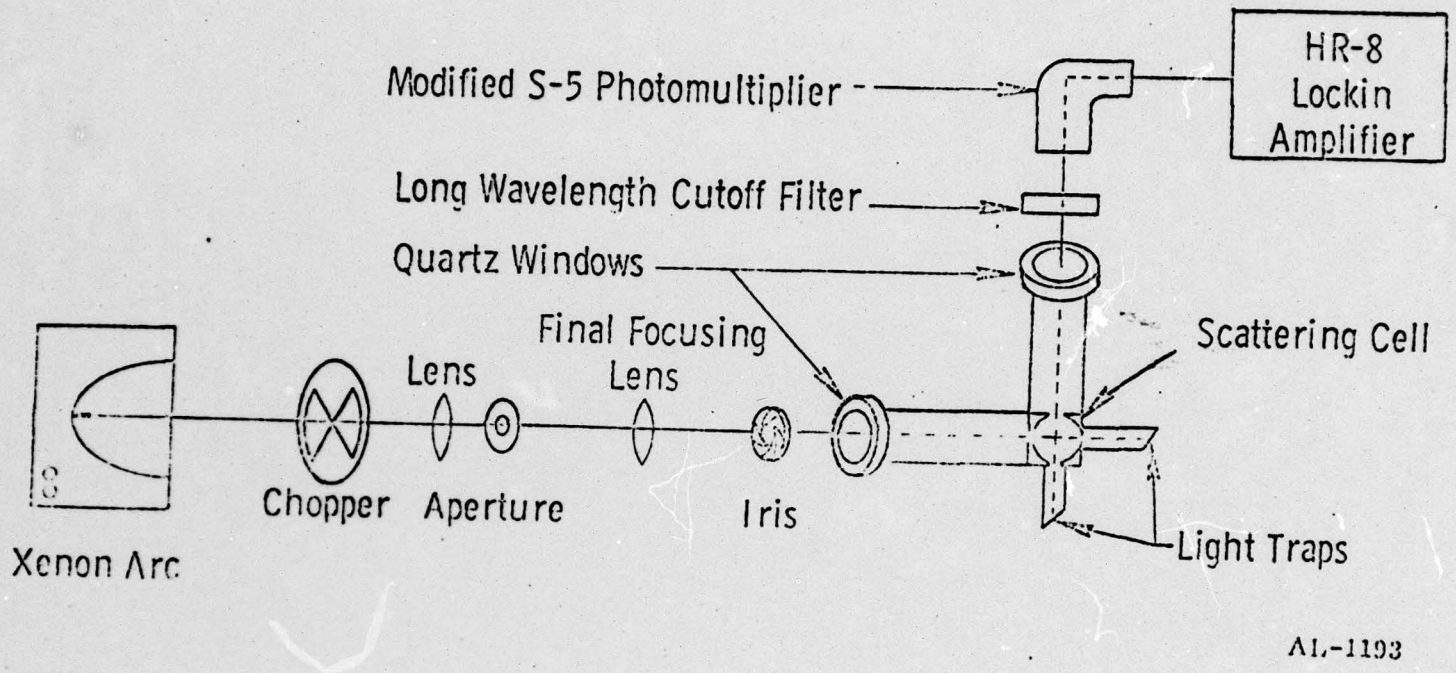

Figure 2

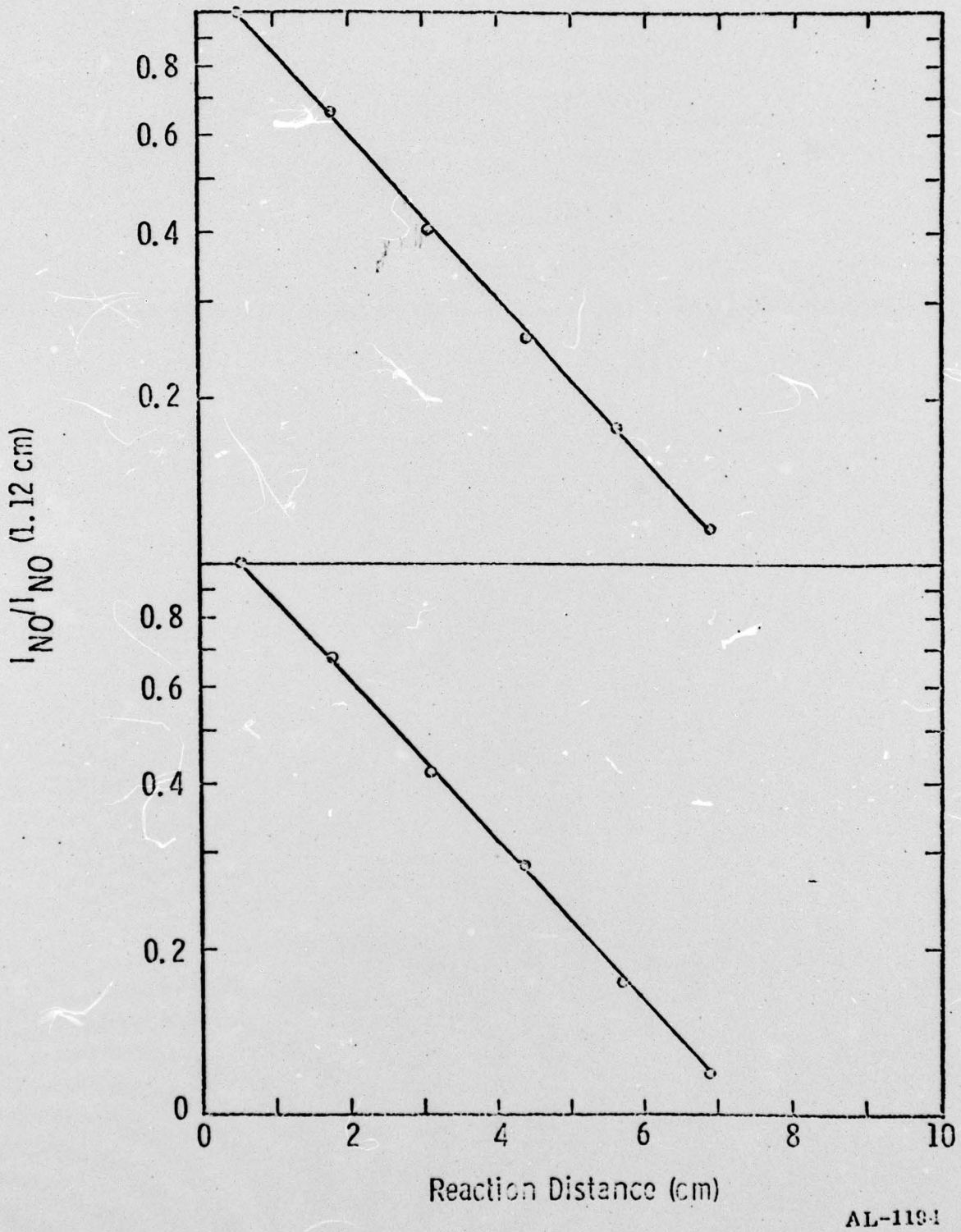

AL-1194

Figure 3

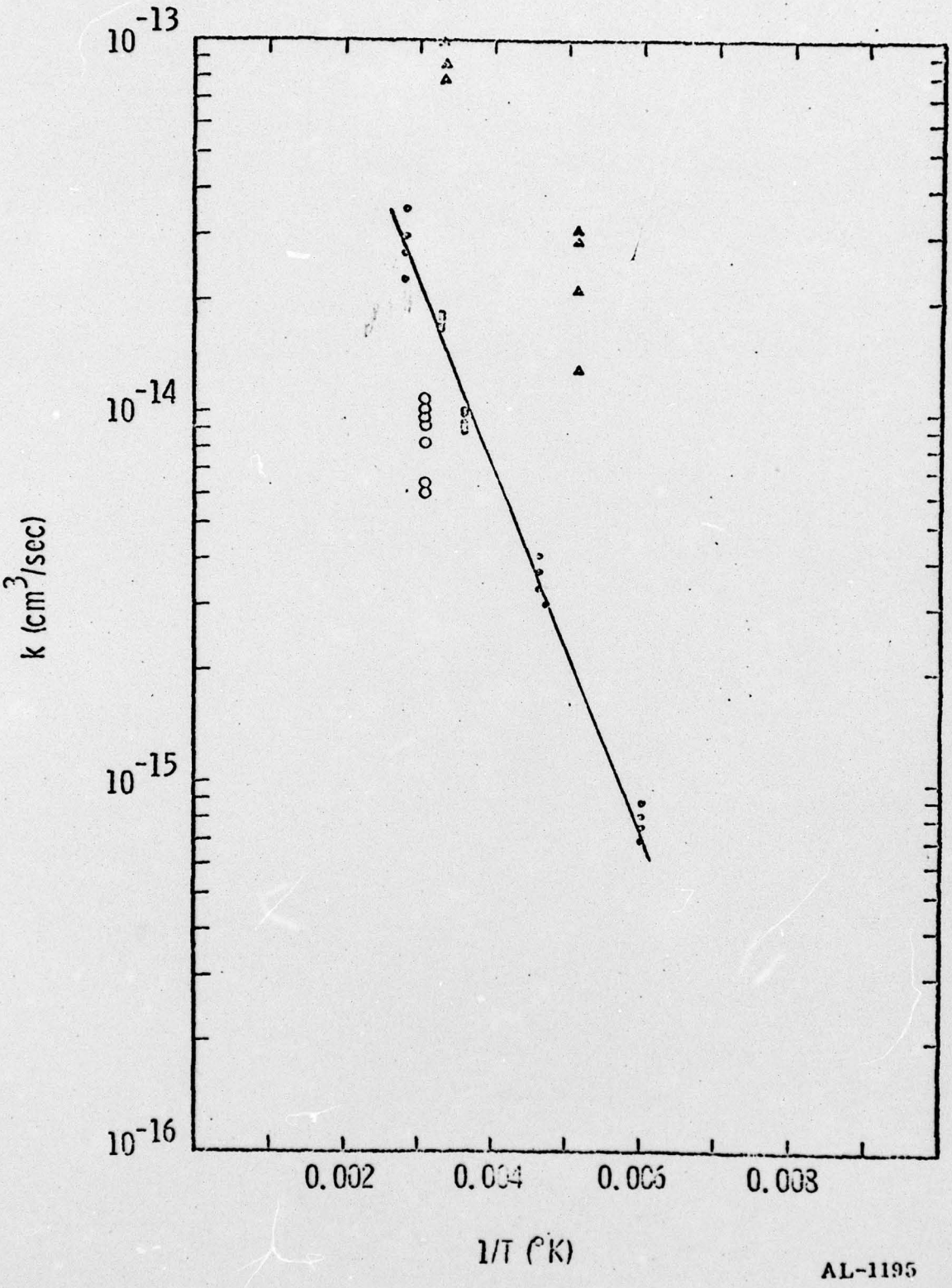

Figure 4